Two Degenerate Boundary Equilibrium Bifurcations in Planar Filippov Systems

SIAM J. Applied Dynamical Systems
Vol. 10, No. 4, pp. 1525–1553

Two Degenerate Boundary Equilibrium Bifurcations in Planar Filippov Systems*

Fabio Dercole†, Fabio Della Rossa†, Alessandro Colombo‡, and Yuri A. Kuznetsov§

Abstract. We contribute to the analysis of codimension-two bifurcations in discontinuous systems by studying all equilibrium bifurcations of 2D Filippov systems that involve a sliding limit cycle. There are only two such local bifurcations: (1) a degenerate boundary focus, which we call the *homoclinic boundary focus* (HBF), and (2) the *boundary Hopf* (BH). We prove that—besides local bifurcations of equilibria and pseudoequilibria—the universal unfolding of the HBF singularity includes a codimension-one global bifurcation at which a *sliding homoclinic orbit to a pseudosaddle* exists, while that of the BH singularity has a codimension-one bifurcation curve along which a cycle *grazing* occurs. We define two *canonical forms*, one for each singularity, to which a generic 2D Filippov system can be locally reduced by smooth changes of variables and parameters and time reparametrization. Explicit genericity conditions are also provided, as well as the asymptotics of the bifurcation curves in the two-parameter space. We show that both studied codimension-two bifurcations occur in a known 2D Filippov system modeling an ecosystem subject to on-off harvesting control, and we provide two *Mathematica* scripts that automatize all computations.

Key words. Filippov systems, bifurcations, codimension-two

AMS subject classifications. 34A36, 34C20, 37G10, 37N35, 93C65

DOI. 10.1137/100812549

1. Introduction.

Bifurcations of discontinuous dynamical systems have received much attention recently, not only as an interesting mathematical topic, but also in applied mathematical modeling of various natural, technical, and social systems (see [2, 6] and references therein). Among discontinuous systems, one of the most studied classes are *Filippov systems* [13, 14] defined by different smooth ODEs in different open domains S_i separated by smooth *discontinuity boundaries*. For these systems, continuous solutions can be constructed by concatenation of standard solutions in S_i's and sliding solutions along the boundaries. We recall this construction briefly for n-dimensional systems depending on modeling and/or control parameters $\alpha \in \mathbb{R}^m$.

Consider two adjacent parameter-dependent domains $S_{1,2} \subset \mathbb{R}^n$,

$$S_1(\alpha) = \{x \in \mathbb{R}^n : H(x,\alpha) < 0\}, \qquad S_2(\alpha) = \{x \in \mathbb{R}^n : H(x,\alpha) > 0\},$$

*Received by the editors October 21, 2010; accepted for publication (in revised form) by T. Seara October 3, 2011; published electronically December 13, 2011.
http://www.siam.org/journals/siads/10-4/81254.html

†Dipartimento di Elettronica e Informazione, Politecnico di Milano, via Ponzio 34/5, 20133 Milano, Italy (fabio.dercole@polimi.it, fabio.dellarossa@mail.polimi.it). The work of these authors was supported by the Ministero dell'Istruzione, dell'Università e della Ricerca (FIRB Futuro in ricerca, project "Modeling and Analysis of Innovation and Competition Processes").

‡Department of Mechanical Engineering, Massachusetts Institute of Technology, 77 Massachusetts Avenue, Cambridge, MA 02139 (acolombo@mit.edu).

§Department of Mathematics, Utrecht University, Budapestlaan 6, 3584 CD Utrecht, The Netherlands (I.A.Kouznetsov@uu.nl).

separated by a smooth $(n-1)$-dimensional boundary $\Sigma(\alpha) = \{x \in \mathbb{R}^n : H(x,\alpha) = 0\}$, where H is a smooth scalar function with nonvanishing gradient $H_x(x,\alpha)$ on $\Sigma(\alpha)$, and assume that

$$\dot{x} = \begin{cases} f^{(1)}(x,\alpha), & x \in S_1(\alpha), \\ f^{(2)}(x,\alpha), & x \in S_2(\alpha), \end{cases} \tag{1.1}$$

where $f^{(1,2)}$ are smooth parameter-dependent vector fields on $\mathbb{R}^n$. (Though $f^{(i)}$ needs to be defined only in S_i, with a smooth extension to Σ, it is convenient for the analysis to assume a global smooth definition.)

Orbits cross Σ at points where the projections of $f^{(1,2)}$ to $H_x(x,\alpha)$ have the same sign. Where the signs are opposite, the system admits a solution that slides on Σ in accordance with the *Filippov vector field*:

$$\dot{x} = (1-\lambda) f^{(1)}(x,\alpha) + \lambda f^{(2)}(x,\alpha), \tag{1.2}$$

with λ being selected so that $\dot{x}$ is tangent to Σ. Sliding is stable (and simply called sliding) when Σ is attracting ($f^{(1,2)}$ push toward Σ), and unstable (called *escaping*) in the opposite case.

The $(n-2)$-dimensional borders between the crossing and sliding regions of Σ are generically composed of *tangency points*, where one of the vector fields $f^{(1,2)}$ is tangent to Σ ($\lambda = 0, 1$ in (1.2), respectively). A tangency point of $f^{(i)}$ is called *visible* if the orbit of $f^{(i)}$ passing through the point locally lies in S_i, and *invisible* otherwise.

Generic equilibria of system (1.1) can be standard equilibria of $f^{(1,2)}$ in $S_{1,2}$ or equilibria of the Filippov vector field with $\lambda \in (0,1)$, called *pseudoequilibria*, where $f^{(1,2)}$ are nonzero and anticollinear. The stability of pseudoequilibria is determined by the Filippov vector field together with the stability of the sliding. Standard equilibria and pseudoequilibria of (1.1) are called *admissible*, while equilibria of $f^{(i)}$ in S_j, $i \neq j$, and equilibria of (1.2) in the crossing region ($\lambda < 0$ or $\lambda > 1$) are called *virtual*. (We refer to [2, 6] for a thorough treatment of Filippov systems.)

Bifurcation analysis of Filippov systems is nontrivial and still patchy. The interaction of the vector fields $f^{(1,2)}$ with the discontinuity boundary requires a proper notion of system equivalence and generates a great number of completely new bifurcations, where the boundary is critically involved (*discontinuity-induced bifurcations*; see [2, 6]). Known results focus on particular orbits, e.g., equilibria or cycles, and only in the case of generic 2D Filippov systems has the classification of all one-parameter bifurcations been proposed [20] (and recently completed in [15]), together with canonical one-parameter bifurcation diagrams. We adopt the definition of a bifurcation from [20].

Most discontinuous models used in applications have several control parameters, and their one-parameter bifurcation diagrams depend strongly on the values of other (fixed) parameters. To understand the rearrangements of one-parameter diagrams, one has to study so-called codimension-two (codim 2 in the following) bifurcations, which serve as organizing centers for two-parameter bifurcation diagrams. In the plane of two control parameters, say α_1 and α_2, curves of codim 1 bifurcations meet (transversally or tangentially) at codim 2 points; thus their analysis determines all possible one-parameter diagrams nearby. This explains the importance of the mathematical analysis of codim 2 bifurcations that is now routinely applied

to smooth dynamical systems, where the essential features of all local codim 2 bifurcations of equilibria and limit cycles are well understood. In contrast, the analysis of codim 2 bifurcations in discontinuous systems has started only recently [10, 16, 17, 22, 15, 8] and is far from being complete, while such bifurcations appear more and more often in applications; see, e.g., [11, 9, 5, 18, 7, 21].

A codim 2 bifurcation of an equilibrium is of particular interest when it involves bifurcations of cycles or other global phenomena, e.g., homoclinic bifurcations. A typical smooth example is the famous Bogdanov–Takens bifurcation (see, e.g., [19]), where the presence of a codim 2 equilibrium with a double zero eigenvalue implies the existence of a limit cycle that is generated by the Hopf bifurcation and disappears via a global saddle homoclinic bifurcation. We expect similar phenomena also in the discontinuous case. Their analysis will provide an analytical method to prove existence of sliding cycles and their global sliding bifurcation of codim 1 in particular models.

In this paper, we contribute to the analysis of codim 2 bifurcations in discontinuous systems by studying all equilibrium (local) bifurcations in 2D Filippov systems that involve codim 1 bifurcations of sliding limit cycles. It follows from the visual inspection of all codim 1 cases treated in [20] that such codim 2 bifurcations can occur only at a degenerate boundary focus (a focus equilibrium of the vector field $f^{(1)}$ or $f^{(2)}$ colliding with the discontinuity boundary). There are actually only two cases, as explained at the end of section 2.1. In one case the focus collides with a visible tangency point and a pseudosaddle and, at the same time, the infinitesimal loop originated at the tangency point merges with the stable manifold of the pseudosaddle. As a result, a small *sliding homoclinic orbit to the pseudosaddle* exists close to the codim 2 bifurcation, and the corresponding codim 1 bifurcation curve emanates from the codim 2 point in the universal local bifurcation diagram. For this reason, we call this codim 2 bifurcation a *homoclinic boundary focus* (HBF). The second degenerate boundary focus is the *boundary Hopf* (BH) bifurcation at which the focus collides with the discontinuity boundary while being at the same time nonhyperbolic. The small-amplitude limit cycle originating through the Hopf bifurcation grazes the discontinuity boundary close to the codim 2 bifurcation, so that a codim 1 grazing bifurcation curve emanates from the codim 2 point at the BH bifurcation.

In both cases (treated in sections 3.2 and 3.3, respectively), starting from a generic 2D Filippov system exhibiting the bifurcation, we derive a canonical form to which the system can be reduced through explicit smooth changes of variables and parameters (and time reparametrization in the BH case) near the codim 2 point. The bifurcation analysis is then performed on the canonical forms and provides explicit genericity conditions expressed in the original variables and parameters. Moreover, leading asymptotics for the global bifurcation curves (sliding homoclinic orbit to pseudosaddle and grazing) are computed in the original parameter space. While the unfolding of the HBF case is new and rather involved, the BH case is easier and has already been addressed in [5] and [15]. As precisely discussed in section 3.3, the unfolding in the first contribution is not generic, while the second is not complete and does not provide means to compute the coefficients of the canonical form explicitly.

We also provide two *Mathematica* scripts (see 81254_01.zip [local/web 30.1KB]), one for each studied codim 2 bifurcation, that automatically check all genericity conditions and compute the bifurcation asymptotics for a generic 2D Filippov system. (The user must provide

the model equations and the numerical values of the boundary equilibrium and parameters at the codim 2 bifurcation.) The scripts are used on a known 2D Filippov system that models a prey-predator ecosystem subject to on-off harvesting control, where both the HBF and BH bifurcations indeed occur (section 4).

We start with a review of the codim 1 bifurcations of 2D Filippov systems that are relevant in section 3. We label with G the genericity conditions that we assume throughout the paper, while we use labels HBF and BH for the genericity conditions that are specific to sections 3.2 and 3.3, respectively.

2. Relevant codim 1 bifurcations of 2D Filippov systems. Here we briefly describe local and global codim 1 bifurcations of 2D Filippov systems, which occur near the codim 2 points in question. The presentation is based on [20] and is included for completeness.

We assume that $\alpha \in \mathbb{R}$ is a small control parameter and that, when $\alpha = 0$, the vector field $f^{(1)}$ has a hyperbolic equilibrium at $x = 0$ lying on Σ, i.e.,

$$(f^{(1)})^0 = 0, \quad H^0 = 0, \quad \operatorname{Re}\lambda^0_{1,2} \neq 0, \tag{G.1}$$

where $\lambda^0_{1,2}$ are the eigenvalues of $(f^{(1)}_x)^0$ and the 0-superscript stands for evaluation at $(x, \alpha) = (0, 0)$. The nonsingularity of $(f^{(1)}_x)^0$ ensures that, through a parameter-dependent translation, we can have

$$f^{(1)}(0, \alpha) = 0, \tag{2.1}$$

i.e., that $x = 0$ is an equilibrium of $f^{(1)}$ for all α in a neighborhood of $\alpha = 0$. We also require the vector field $f^{(2)}$ to be locally transverse to Σ, i.e.,

$$H^0_x (f^{(2)})^0 \neq 0, \tag{G.2}$$

and the transversality of the codim 1 boundary equilibrium (BE) bifurcation, i.e.,

$$H^0_\alpha \neq 0, \tag{G.3}$$

e.g., $H^0_\alpha > 0$, so that $x = 0$ is admissible for $\alpha < 0$ and virtual for $\alpha > 0$.

As explained in [4], it is known that generic BE bifurcations can be classified into two scenarios: (a) *persistence* when the standard equilibrium collides with the discontinuity boundary and turns into a pseudoequilibrium, and (b) *nonsmooth-fold* when the standard equilibrium and a coexisting pseudoequilibrium collide and disappear through the bifurcation. The conditions to distinguish the two scenarios (derived in [4]; see [10] for a geometric interpretation) are

$$\text{persistence: } H^0_x((f^{(1)}_x)^0)^{-1}(f^{(2)})^0 > 0, \tag{2.2a}$$

$$\text{nonsmooth-fold: } H^0_x((f^{(1)}_x)^0)^{-1}(f^{(2)})^0 < 0, \tag{2.2b}$$

and the codim 2 bifurcation at which the left-hand side in (2.2) vanishes, called the *generalized* BE, has recently been studied for n-dimensional Filippov systems in [10]. (A fold bifurcation

between pseudoequilibria has been shown to concomitantly occur and the corresponding bifurcation curve emanates from the codim 2 point tangentially to the BE curve; we will come back to this point in section 4.) Generically, we therefore have

$$H_x^0((f_x^{(1)})^0)^{-1}(f^{(2)})^0 \neq 0. \tag{G.4}$$

Finally, in this section, we assume that the discontinuity boundary is locally horizontal ($H_x(x,\alpha) = [0,\,1]^\top$, i.e., S_1 (S_2) is below (above) the boundary), and that the vector field $f^{(2)}$ is locally nonzero and orthogonal to the discontinuity boundary (i.e., vertical), so that the state portrait in S_2 is trivial, while all essential events happen on Σ and in S_1. This can be done without loss of generality thanks to the change of variables proposed in [20, section 3.1] and fully described in Appendix A.

For simplicity of presentation, we consider only cases where sliding is stable (no escaping, vector field $f^{(2)}$ points downward, i.e., $H_x^0(f^{(2)})^0 < 0$ in (G.2)) and rotations are counterclockwise. Reversing the direction of time and/or that of the x_1-axis reduces all other cases to the considered ones.

2.1. Boundary focus (BF) bifurcations. A standard focus equilibrium of the vector field $f^{(1)}$ hits the discontinuity boundary Σ at $\alpha = 0$. (Since the equilibrium is $x = 0$ for any small $|\alpha|$, it is actually the discontinuity boundary that moves with α.) Assuming stable sliding and counterclockwise rotations nearby, there are five generic BF scenarios: BF_i, $i = 1, \ldots, 5$. The cases are distinguished by the stability of the focus, the relative position of its zero-isoclines, and the behavior of the orbit departing from the visible tangency point into S_1. The unfoldings of these singularities are sketched in Figure 1.

In case BF_1, a stable sliding cycle L surrounds the unstable focus O for $\alpha < 0$. The sliding segment of the cycle ends at the visible tangency point T and begins at a transverse arrival point located between T and a pseudosaddle P. The domain of attraction of this cycle is bounded by the stable manifold of P. When $\alpha \to 0$, the stable cycle shrinks, while points O, T, and P collide simultaneously. For small $\alpha > 0$, there are no equilibria or cycles, and the stable sliding orbit begins at the invisible tangency point T. This bifurcation entails the catastrophic disappearance of a stable sliding cycle.

In case BF_2, the orbit departing from the visible tangency point T for small $\alpha < 0$ returns to Σ on the right of the pseudosaddle P. Thus, no sliding cycle exists. The state portraits for $\alpha \geq 0$ are like those in case BF_1.

In case BF_3, a stable sliding cycle L surrounds the unstable focus O for $\alpha < 0$. Contrary to case BF_1, there is no pseudoequilibrium nearby. When $\alpha \to 0$, the stable cycle shrinks and the focus collides with the tangency point T. For small $\alpha > 0$, there is no cycle, and all nearby orbits tend to a stable pseudoequilibrium P that exists close to the invisible tangency point T. This bifurcation implies the noncatastrophic disappearance of a stable sliding cycle.

In case BF_4, the focus O is stable and attracts all nearby standard and sliding orbits for small $\alpha < 0$. When $\alpha \to 0$, the focus O collides with the tangency point T. The state portraits for $\alpha \geq 0$ are like those in case BF_3.

In the last case BF_5, the domain of attraction of the stable focus O is bounded for $\alpha < 0$ by the stable manifold of a pseudosaddle P. When $\alpha \to 0$, points O, T, and P collide simultaneously. The state portraits for $\alpha \geq 0$ are like those in case BF_1.

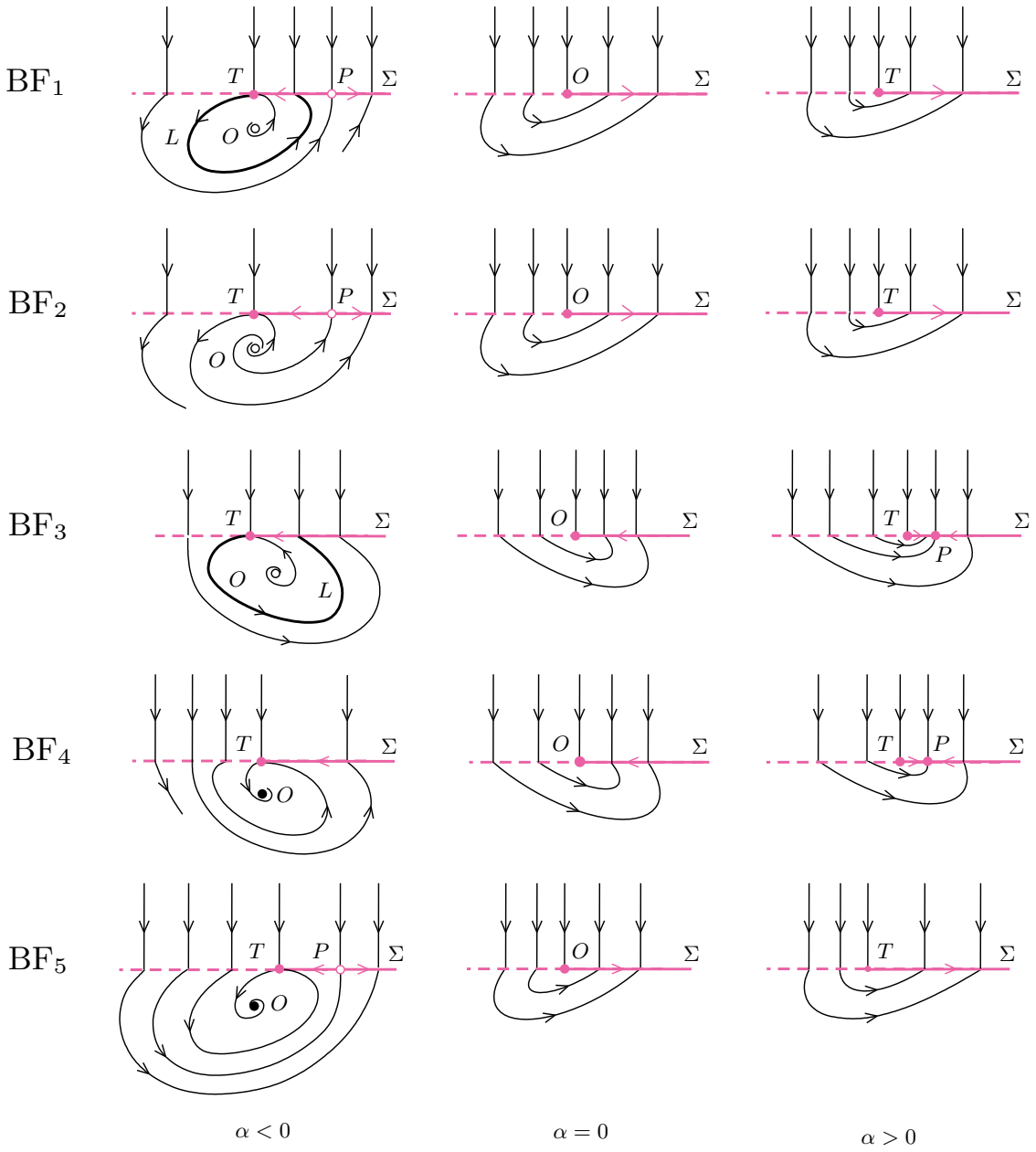

Figure 1. *Five types of generic codim* 1 BF *bifurcations in* 2*D Filippov systems: In cases* BF_1 *and* BF_3 *stable sliding cycles exist for nearby parameter values. The figure is adapted from* [20, Fig. 5]*, where escaping is considered in cases* BF_4 *and* BF_5.

Note that we have the persistence BE scenario in cases BF_3 and BF_4, while the nonsmooth-fold BE scenario occurs in cases BF_1, BF_2, and BF_5.

We can now identify the codim 2 BF bifurcations at which a codim 1 bifurcation of a

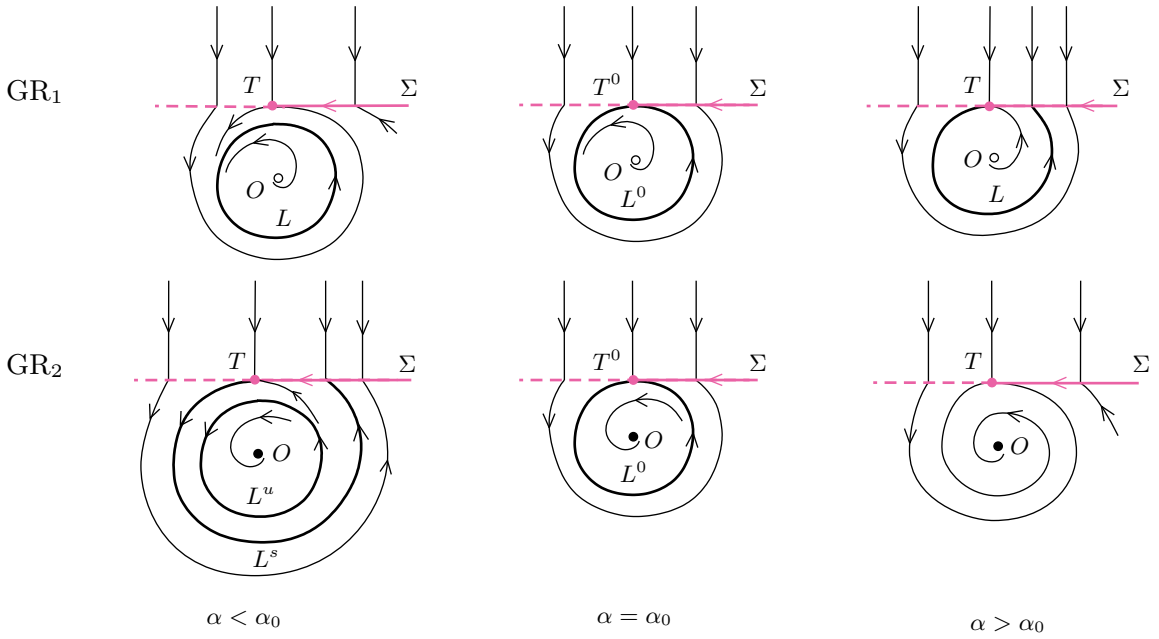

Figure 2. *Two types of* GR *bifurcations in* 2*D Filippov systems (adapted from* [20, Fig.14]*).*

sliding cycle is also involved. As shown in [10], no sliding cycle bifurcations can generically occur at a generalized BE (the change between persistence and nonsmooth-fold), so that all transitions between one of $BF_{3,4}$ and one of $BF_{1,2,5}$ are excluded. We therefore study the transition BF_1–BF_2 (HBF) and the transitions BF_3–BF_4 and BF_1–BF_5 (BH in the persistence and nonsmooth-fold BE scenarios, respectively), while the BH analysis shows that transition BF_2–BF_5 is generically not possible.

2.2. Grazing bifurcation. A standard cycle in S_1 touches tangentially the discontinuity boundary Σ at $\alpha = \alpha_0$ near $\alpha = 0$ (recall that the equilibrium $x = 0$ inside the cycle hits the boundary at $\alpha = 0$). This phenomenon is called the *grazing* bifurcation (GR). Two generic bifurcation scenarios $GR_{1,2}$ are possible here, depending on the stability of the grazing cycle L^0. In case GR_1 the cycle L^0 is stable, while it is unstable in case GR_2.

The unfolding of the $GR_{1,2}$ singularities are presented in Figure 2 (note that, being close to a BE bifurcation at $\alpha = 0$, no other cycles are contained in L). In case GR_1, there is a stable cycle $L \subset S_1$ for $\alpha < \alpha_0$. Then, for $\alpha > \alpha_0$, L becomes a stable sliding cycle (persistence scenario for cycles; see [3]). In case GR_2, two cycles exist for $\alpha < \alpha_0$: an unstable standard cycle $L^u \subset S_1$ and a stable sliding cycle L^s. These cycles coalesce at $\alpha = \alpha_0$, forming a grazing cycle. For $\alpha > \alpha_0$, no cycles exist nearby (nonsmooth-fold scenario).

Unfoldings $GR_{1,2}$ refer to the persistence scenario of the BE bifurcation at $\alpha = 0$. A pseudosaddle, not involved in the grazing bifurcation at $\alpha = \alpha_0$, must exist close to the tangency point T in the BE nonsmooth-fold scenario (see point P in the panels across the $GR_{1,2}$-curves in the bottom part of Figure 6).

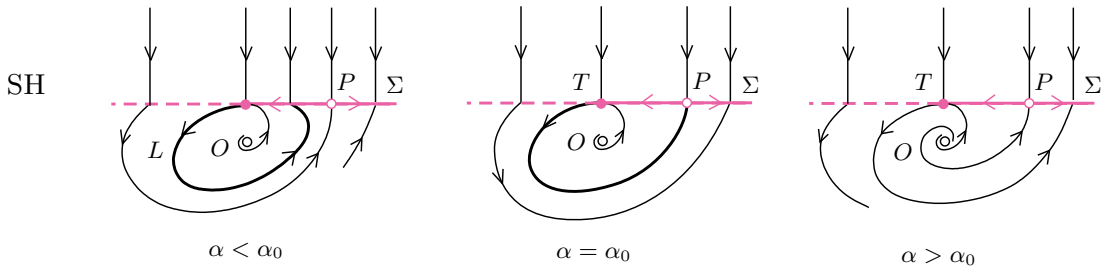

Figure 3. SH *bifurcation in* 2*D Filippov systems (adapted from* [20, Fig. 19]*).*

2.3. Sliding homoclinic orbit to pseudosaddle. A sliding cycle L with standard segment in S_1 exists, say for $\alpha < \alpha_0 \neq 0$, and collides with a pseudosaddle at $\alpha = \alpha_0$ (as before, the equilibrium $x = 0$ inside the cycle hits the boundary at $\alpha = 0$). The generic bifurcation diagram is shown in Figure 3. The state portraits at $\alpha \lessgtr \alpha_0$ are equivalent to those in the left column of Figure 1, cases BF_1 and BF_2, while the orbit from the tangency point T reaches the pseudosaddle P when $\alpha = \alpha_0$. There is no periodic orbit for $\alpha > \alpha_0$. This bifurcation (labeled SH) is analogous to the homoclinic bifurcation to standard saddle.

3. Main results. In this section we derive our original results, namely the unfoldings of two codim 2 bifurcations. In section 3.2 we unfold the homoclinic boundary focus (HBF), occurring at the border between BF_1 and BF_2 cases described in section 2.1, while in section 3.3 we treat the boundary Hopf (BH), a focus on the discontinuity boundary with purely imaginary eigenvalues (transitions BF_3–BF_4 and BF_1–BF_5). As in section 2, with no loss of generality, we consider stable sliding (i.e., $H^0_x(f^{(2)})^0 < 0$ in (G.2)) and counterclockwise rotations. We first present a change of variables and parameters that will be useful in the analysis of both singularities.

3.1. A useful change of variables and parameters. As anticipated in section 2, we can introduce new variables $z = [z_1, z_2]^\top$ that locally make the discontinuity boundary flat and horizontal and the vector field $f^{(2)}$ constant and vertical (see [20, sect. 3.1]; details are reported in Appendix A). The idea is to define a smooth parametrization z_1 of the discontinuity boundary Σ, with $z_1 = 0$ corresponding to the intersection with Σ of the $f^{(2)}$-orbit passing through the equilibrium $x = 0$ of the vector field $f^{(1)}$ (this is possible thanks to assumption (G.2)). For each small $\|x\|$, we associate with x the z_1-value at the intersection with Σ of the $f^{(2)}$-orbit through x, and let $\tau_2(x, \alpha)$ be the time taken by the orbit to go from x to Σ (positive if $x \in S_2$; negative if $x \in S_1$; zero if x is on Σ). We then set $z_2 = \tau_2(x, \alpha) - \tau_2(0, \alpha)$, so that $x = 0$ is mapped into $z = 0$. In this way, points x on the discontinuity boundary have constant z_2, while points along an $f^{(2)}$-orbit in S_2 have the same z_1; i.e., the orbit is vertical in the new variables. Moreover, as x approaches Σ, the time to reach Σ, i.e., z_2, decreases with the "speed of time," so that $\dot{z}_2 = -1$.

We therefore obtain the system

$$\dot{z} = \begin{cases} f(z, \alpha), & z_2 < -\tau_2(0, \alpha), \\ [0, -1]^\top, & z_2 > -\tau_2(0, \alpha), \end{cases} \tag{3.1}$$

where f is nothing but the vector field $f^{(1)}$ in the new variables, with $f(0,\alpha)=0$. Let us write

$$f(z,\alpha)=J(\alpha)\,z+O(\|z\|^2),\quad J(\alpha)=\begin{bmatrix} a(\alpha) & b(\alpha)\\ c(\alpha) & d(\alpha)\end{bmatrix}, \tag{3.2}$$

where explicit expressions for functions a, b, c, d, and their α-derivatives are given in Appendix A (see (A.12) and (A.14)).

Introduce now two new parameters

$$\beta_1=\beta_1(\alpha):=-\tau_2(0,\alpha)\quad\text{and}\quad \beta_2=\beta_2(\alpha),\quad\text{with}\quad \beta_2^0=0, \tag{3.3}$$

such that close to $\alpha=0$ the map $\beta=\beta(\alpha)$ is invertible, i.e., the 2×2 Jacobian β_α^0 is nonsingular. (Function $\beta_2(\alpha)$ takes different forms in sections 3.2 and 3.3.) Then, β_1 is the distance of the equilibrium $z=0$ from Σ (the equation of the boundary becomes $z_2-\beta_1=0$), and the BF bifurcation curve has equation $\beta_1=0$ (β_2-axis), with the equilibrium $z=0$ admissible for $\beta_1>0$ and virtual for $\beta_1<0$.

3.2. Homoclinic boundary focus. The first codim 2 bifurcation that we study, HBF, occurs at the border between cases BF_1 and BF_2 described in section 2.1. Here $\alpha\in\mathbb{R}^2$, $\alpha=0$ being the codim 2 point, and we keep assumptions (G.1)–(G.4) and the parameter-dependent translation ensuring (2.1). Note that (G.3) now says that the codim 1 BF bifurcation curve is well defined, locally to $\alpha=0$ in the parameter plane (α_1,α_2), by $H(0,\alpha)=0$ and has a nonvanishing gradient H_α^0 at $\alpha=0$.

We study system (3.1) in the nonsmooth-fold BE scenario at $(z,\alpha)=(0,0)$, so that we replace (G.4) with

$$\begin{bmatrix}0 & 1\end{bmatrix}\frac{1}{\det J^0}\begin{bmatrix} d^0 & -b^0\\ -c^0 & a^0\end{bmatrix}\begin{bmatrix}0\\-1\end{bmatrix}=-\frac{a^0}{\det J^0}<0, \tag{HBF.4}$$

and we assume that $z=0$ is a focus of the vector field f in (3.2) at $\alpha=0$; i.e., we assume

$$\Delta^0<0, \tag{HBF.5}$$

where

$$\Delta(\alpha):=(a(\alpha)-d(\alpha))^2+4\,b(\alpha)\,c(\alpha). \tag{3.4}$$

Moreover, for the sliding to be stable, cases BF_1 and BF_2 require an unstable focus, and we consider counterclockwise rotations, so that we further assume

$$\mathrm{tr}J^0=a^0+d^0>0\quad\text{and}\quad b^0<0, \tag{3.5}$$

and $c^0>0$ due to (HBF.5). Note that (HBF.5) also implies

$$\det J^0=a^0d^0-b^0c^0>0, \tag{3.6}$$

so that (HBF.4) simply reduces to $a^0>0$.

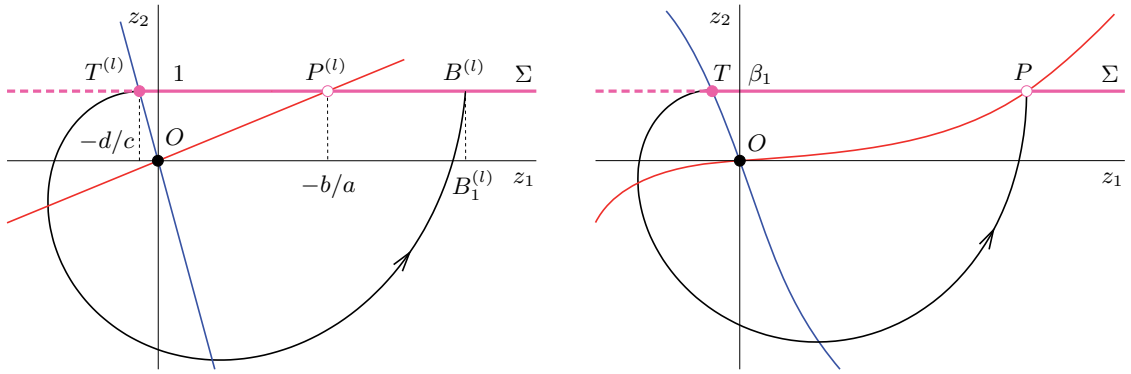

Figure 4. *Left: Construction of function $\psi(z_1, \alpha)$. Right: Sliding homoclinic orbit to the pseudosaddle in system (3.1). Red (blue) lines: z_1 (z_2)-zero-isoclines.*

As a first step in the analysis, we define a smooth test function $\varphi(\alpha)$ that along the BF bifurcation curve (i.e., when $H(0, \alpha) = 0$) is positive in case BF_1 and negative in case BF_2. Let us do this for the linearized system, namely system (3.1) with the dynamics below the discontinuity boundary replaced by

$$\dot{z} = J(\alpha)\, z. \tag{3.7}$$

(We use an (l)-superscript to denote quantities characterizing the linearized system that have a counterpart in the nonlinear one.) We later show that $\varphi(\alpha)$ is also a test function for the full nonlinear system.

Most of the details are relegated to Appendix B.1, where we define a function $\psi(z_1, \alpha)$ such that $\psi(B_1^{(l)}(\alpha), \alpha) = 0$ uniquely defines the value $B_1^{(l)}(\alpha)$ of z_1 at which the orbit of system (3.7), starting at the tangency point

$$T^{(l)}(\alpha) := [-d(\alpha)/c(\alpha),\ 1]^\top, \tag{3.8}$$

first goes back to the discontinuity boundary $z_2 = 1$ (see Figure 4(left)), with $\psi(z_1, \alpha) \gtrless 0$ for $z_1 \gtrless B_1^{(l)}$. The choice of the boundary $z_2 = 1$ is here arbitrary. In fact, we are interested to know whether the orbit in Figure 4(left) returns to Σ on the left or on the right of the pseudosaddle,

$$P^{(l)}(\alpha) := [-b(\alpha)/a(\alpha),\ 1]^\top, \tag{3.9}$$

and considering a different boundary $z_2 = \tilde{z}_2$ would simply scale the figure (due to the linearity of the system). Thus, the figure remains unchanged (by consistently scaling the z-axes) also in the limit $\tilde{z}_2 \to 0$, i.e., at the BF bifurcation, where we need to evaluate our test function.

The result for the linearized system is that BF_1 (BF_2) is the case in which $B_1^{(l)}$ is less (greater) than $-b/a$, i.e.,

$$\varphi(\alpha) := \psi(-b(\alpha)/a(\alpha), \alpha) \begin{cases} > 0, & \mathrm{BF}_1, \\ = 0, & \mathrm{HBF}, \\ < 0, & \mathrm{BF}_2, \end{cases} \tag{3.10}$$

and we require that $\varphi(\alpha)$ generically change sign with nonzero slope when α moves through $\alpha = 0$ along the BF curve, i.e.,

$$\varphi^0 = 0 \quad \text{and} \quad \langle \varphi^0_\alpha, (H^\perp_\alpha)^0 \rangle \neq 0, \tag{HBF.6}$$

where $H^\perp_\alpha := [H_{\alpha_2}, -H_{\alpha_1}]$ is tangent to the BF curve ($\pi/2$-clockwise-rotated w.r.t. H_α) and $\langle \cdot, \cdot \rangle$ denotes the standard scalar product in $\mathbb{R}^2$.

The explicit expression for φ comes from Appendix B.1 (see (B.10) for the expression of ψ) and reads

$$\varphi(\alpha) := \frac{\omega}{a+d} \log\left(-\frac{bc}{a^2}\right) - \arctan(d-a, 2\omega) - \pi, \quad \omega := \frac{\sqrt{-\Delta}}{2}, \tag{3.11}$$

where Δ is defined in (3.4) and the α-dependence is confined in a, b, c, d, and ω, while the α-derivatives in (HBF.6) (and later in (3.18)) can be easily computed as the derivatives of (3.11) w.r.t. a–d and taking the α-derivatives of a–d from Appendix A (see (A.14)). Note that on the curve $\varphi(\alpha) = 0$, the linearized system has a sliding homoclinic orbit. We can therefore expect that this happens if and only if the nonlinear system (3.1) has a sliding homoclinic (SH) bifurcation emanating from $\alpha = 0$. We now show that this is indeed the case, hence confirming that $\varphi(\alpha)$ is the test function we were looking for.

Let us complete the parameter change (3.3) with

$$\beta_2 = \beta_2(\alpha) := \varphi(\alpha) \tag{3.12}$$

and note that (HBF.6) ensures invertibility (take the second equation of (A.5) into account).

In the new variables and parameters (z, β), the SH bifurcation curve is implicitly defined as follows (see Figure 4(right)). Let $z(t) = \Phi(z(0), t, \alpha(\beta))$ be the flow generated by the vector field f in (3.1). Under (HBF.5) and (3.5), locally to $(z, \beta) = (0, 0)$ and for $\beta_1 \neq 0$, the time $\tau(\beta)$ needed by Φ to go from the tangency point $T(\beta)$ close to $z = 0$ back to the discontinuity boundary is well defined, i.e.,

$$\Phi_2(T(\beta), \tau(\beta), \alpha(\beta)) = \beta_1. \tag{3.13}$$

By contrast, when $\beta_1 = 0$, the tangency point T coincides with the equilibrium $z = 0$, and τ is undetermined. By continuity, we fix $\tau(\beta)|_{\beta_1=0}$ at the value required by the linear system (3.7) to go from $T^{(l)}$ back to the boundary $z_2 = 1$ (see Figure 4(left)), i.e.,

$$\left(\exp(J(\alpha(\beta))\,\tau(\beta))\,T^{(l)}(\alpha(\beta))\right)_2\Big|_{\beta_1=0} = 1. \tag{3.14}$$

(The 2-subscript stands for the second element; see (C.9) for an explicit formula at $\beta = 0$.)

The SH connection requires that the f-orbit starting at T go back to Σ at the pseudosaddle P, which is a point of the z_1-zero-isocline, i.e.,

$$s(\beta) := f_1(\Phi(T(\beta), \tau(\beta), \alpha(\beta)), \alpha(\beta)) = 0. \tag{3.15}$$

However, (3.15) has the trivial solution $\beta_1 = 0$, where T coincides with $z = 0$ (and with P). This implies that the expansion of $s(\beta)$ has the form

$$s(\beta) = \beta_1 \left(s_{10} + \tfrac{1}{2}\, s_{20}\beta_1 + s_{11}\beta_2 + O(\|\beta\|^2)\right), \tag{3.16}$$

so that a necessary and sufficient condition for the existence of the SH bifurcation curve close to $\beta = 0$ is that $s_{10} = 0$. In Appendix C we indeed show that this is the case if and only if $\varphi^0 = 0$, while generically s_{20} and s_{11} are nonzero, so that the SH curve passes through $\beta = 0$ with linear asymptotic

$$\tfrac{1}{2}\, s_{20}\beta_1 + s_{11}\beta_2 \simeq 0. \tag{3.17}$$

It turns out that s_{11} depends only on the linear term of f in (3.2) and is nonzero under conditions (HBF.4) and (HBF.6), while s_{20} also depends on the quadratic terms. Thus, the linear asymptotic (3.17) does not generically coincide with that of the SH bifurcation curve $\varphi(\alpha) = 0$ of the linearized system, but both asymptotics are transverse to the β_2-axis, i.e., to the BF bifurcation. Of course, only the branch with $\beta_1 > 0$ (along which $z = 0$ is admissible) corresponds to an SH bifurcation for system (3.1), while the asymptotic (3.17) in the original α-parameter plane is simply

$$(-\tfrac{1}{2}\, s_{20}\tau^0_{2\alpha_1} + s_{11}\varphi^0_{\alpha_1})\alpha_1 + (-\tfrac{1}{2}\, s_{20}\tau^0_{2\alpha_2} + s_{11}\varphi^0_{\alpha_2})\alpha_2 \simeq 0, \tag{3.18}$$

where explicit expressions for $\tau^0_{2\alpha}$ and φ^0_α in terms of the original functions H and $f^{(1,2)}$ can be found in Appendix A (see the second equation of (A.5)) and following the text below (3.11), respectively.

Close to $\beta = 0$ there are generically (i.e., under (G.1)–(G.3) and (HBF.4)–(HBF.6)) no other bifurcations. In fact, the equilibrium $z = 0$ remains hyperbolic, and the BE scenario (nonsmooth-fold) does not change (due to (HBF.4)) for small $\|\beta\|$. Thus, there is a unique equilibrium ($z = 0$) and a unique pseudoequilibrium (P) involved in the HBF bifurcation, and the only possible global bifurcation is the SH bifurcation that we have discussed.

In conclusion, we have proved the following result.

Theorem HBF. *Suppose that for a planar Filippov system (1.1) the following assumptions hold at $\alpha = 0$:*

- (G.1) *the vector field $f^{(1)}$ has a hyperbolic equilibrium at $x = 0$ lying on Σ, i.e., $(f^{(1)})^0 = 0$, $H^0 = 0$, $\operatorname{Re}\lambda^0_{1,2} \neq 0$;*
- (G.2) *the vector field $f^{(2)}$ is transverse to Σ at $x = 0$, i.e., $H^0_x(f^{(2)})^0 \neq 0$;*
- (G.3) *the BE bifurcation is locally well defined, i.e., $H^0_\alpha \neq 0$;*
- (HBF.4) *the BE exhibits the nonsmooth-fold scenario, i.e., $H^0_x((f^{(1)}_x)^0)^{-1}(f^{(2)})^0 < 0$;*
- (HBF.5) *$x = 0$ is a focus, i.e., $(\operatorname{tr}(f^{(1)}_x)^0)^2 - 4\det(f^{(1)}_x)^0 < 0$;*
- (HBF.6) *the BE changes from BF_1 to BF_2, i.e., $\varphi^0 = 0$ and $\langle\varphi^0_\alpha, (H^\perp_\alpha)^0\rangle \neq 0$ (see (3.11)).*

Then, by applying a smooth and invertible transformation of coordinate and parameters, $z = z(x,\alpha)$, $\beta = \beta(\alpha)$, system (1.1) can be reduced to the canonical form

$$\dot z = \begin{cases} J(\alpha(\beta))z + f_{zz}(0,\alpha(\beta))(z,z) + O(\|z^3\|), & z_2 < \beta_1, \\ [0,\,-1]^\top, & z_2 > \beta_1, \end{cases}$$

where, independently on O-terms, locally to $\beta = 0$, the β_2-axis is the BE bifurcation ($\mathrm{BF}_{1,2}$ if $\beta_2 \gtrless 0$), while an SH bifurcation curve emanates from $\beta = 0$ for $\beta_1 \geq 0$ with linear asymptotic (3.17) ((3.18) in the original parameters). No other bifurcation is rooted at $\beta = 0$.

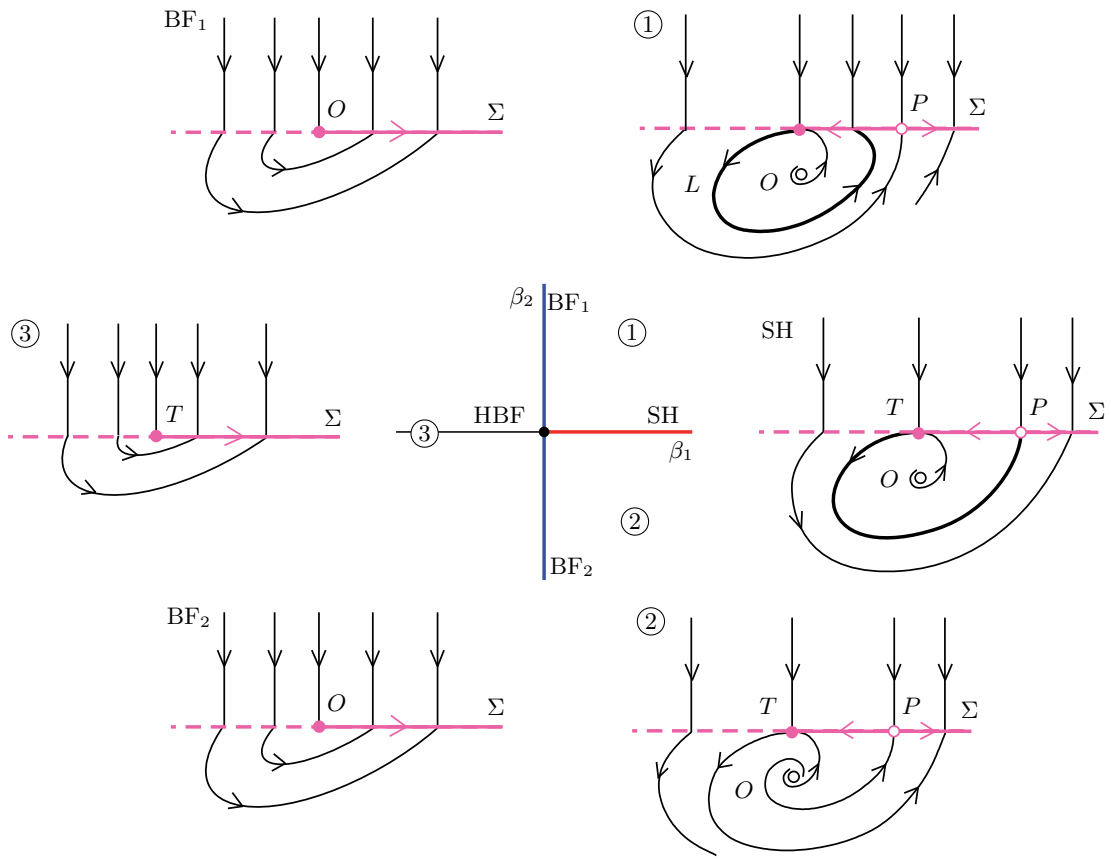

Figure 5. HBF *universal local bifurcation diagram.*

The bifurcation diagram of the HBF singularity locally to $\beta = 0$ is hence that of Figure 5, where the positive (negative) β_2-axis is the BF_1 (BF_2) branch (due to the choice of β_2 in (3.12)), while a linear parameter change makes the SH bifurcation correspond to the positive β_1-semiaxis. The labeling of the corresponding state portraits is in accordance with Figure 1.

3.3. Boundary Hopf. The second codim 2 bifurcation that we consider, BH, occurs at the border between cases BF_3 and BF_4 (in the persistence BE scenario) and BF_1 and BF_5 (nonsmooth-fold BE scenario) described in section 2.1. As in section 3.2, $\alpha \in \mathbb{R}^2$ and $\alpha = 0$ is the codim 2 point. Here we keep assumptions (G.2)–(G.4), while (G.1) is replaced by

$$(BH.1) \qquad (f^{(1)})^0 = 0, \quad H^0 = 0, \quad \lambda^0_{1,2} = \pm i\omega^0 \neq 0,$$

where the nonsingularity of the Jacobian of $f^{(1)}$ at $(x, \alpha) = (0, 0)$ is enough to ensure (2.1). Thus, close to $\alpha = 0$, $x = 0$ is the equilibrium of $f^{(1)}$, and we let $\lambda_{1,2}(\alpha) = \mu(\alpha) \pm i\omega(\alpha)$ be the eigenvalues of $f^{(1)}(0, \alpha)$, with $\mu^0 = 0$ and $\omega^0 > 0$. We further assume the transversality and genericity of the Hopf bifurcation, i.e.,

$$(BH.5) \qquad \mu^0_\alpha \neq 0 \quad \text{and} \quad l^0_1 \neq 0,$$

respectively, where l_1^0 is the first Lyapunov coefficient of the Hopf normal form at the bifurcation (see, e.g., [19, sect. 3.5]).

Under (BH.5), we can reduce the vector field $f^{(1)}$ to Hopf normal form (through smooth and invertible changes of variables and parameters and time reparametrization). We can therefore study the system

$$\dot{y} = \begin{cases} \begin{bmatrix} \beta_2 & -1 \\ 1 & \beta_2 \end{bmatrix} y + l_1(\beta)\|y\|^2 y + O(\|y\|^4), & y_2 < \beta_1(1 + O(\|\beta\|)) + O(\|y\|^2), \\ v(\beta) + O(\|y\|), & y_2 > \beta_1(1 + O(\|\beta\|)) + O(\|y\|^2), \end{cases} \tag{3.19}$$

where $y = y(x, \alpha)$ is the change of variables ($x(y, \alpha)$ being the inverse transformation),

$$\beta_2(\alpha) := \mu(\alpha)/\omega(\alpha) \tag{3.20}$$

completes the parameter change (3.3), and the dot notation now stands for the time-derivative w.r.t. the new time (β-dependence of O-terms is not indicated for simplicity).

Note that, unlike in (3.1), in (3.19) we no longer have a flat discontinuity boundary orthogonal to the $f^{(2)}$-orbits, since $f^{(1)}$ is reduced to Hopf normal form. The best we can do is rotate the axes to make horizontal the linear part of the boundary, because the Hopf normal form is invariant under rotations, but we cannot eliminate the quadratic terms in the boundary expansion, nor the linear terms in the $f^{(2)}$ expansion. Neither can we assume $v^0 = v(0)$ to be vertical, since writing (G.4) in the new variables, we get

$$\begin{bmatrix} 0 & 1 \end{bmatrix} \begin{bmatrix} 0 & 1 \\ -1 & 0 \end{bmatrix} v^0 = -v_1^0 \neq 0.$$

A vertical v^0 would lead to a further degeneracy (generalized BE, the change between persistence and nonsmooth-fold). Obviously, we also cannot have v^0 horizontal, since this would violate (G.2).

As for the new parameters, we already discussed in section 3.1 that the choice of β_1 in (3.3) makes $\beta_1 = 0$ (the β_2-axis) identify the BF bifurcation, while β_2 in (3.20) is the unfolding parameter of the (one-parameter) Hopf normal form; i.e., $\beta_2 = 0$ (the β_1-axis) is the Hopf bifurcation. Of course, we require the invertibility of the parameter change, i.e.,

$$\langle (H_\alpha^\perp)^0, \mu_\alpha^0 \rangle \neq 0 \tag{BH.6}$$

(where $H_\alpha^\perp := [H_{\alpha_2}, -H_{\alpha_1}]$ and the second equation of (A.5) has been used); namely, we assume that the BF and Hopf bifurcation curve transversally intersect at $\alpha = 0$ in the α-parameter plane.

Conditions (BH.1), (G.2)–(G.4), (BH.5), and (BH.6) characterize a generic BH bifurcation. As mentioned in the introduction, two simple Filippov systems have already been proposed to unfold the BH bifurcation [5, 15]. In [5], however, a vertical v^0 is assumed in (3.19), so that a generalized BE bifurcation concomitantly occurs. Indeed, as expected from the unfolding in [10], a fold bifurcation curve between pseudoequilibria emanates from the BH point tangentially to the BF curve (see Figure 5 in [5]). In contrast, the unfolding of the BH

bifurcation in [15] is generic, but considers only the persistence BE scenario. Moreover, no explicit means to compute the coefficients of the proposed canonical form is provided.

We now study the bifurcations of system (3.19) locally to $\beta = 0$. Besides the BF and Hopf bifurcations, there are generically no other local bifurcations. In contrast there are two candidate global bifurcations. The first is the grazing (GR) of the limit cycle originating through the Hopf bifurcation. The second possibility one can imagine in the nonsmooth-fold BE scenario (see (2.2)) is the SH bifurcation occurring when the tangency point close to $y = 0$ is connected with the pseudosaddle colliding with $y = 0$ at the BF. This is, however, generically not possible. In fact, by changing variables from x to z as described in section 3.1, we can consider system (1.1) in the form (3.1) (with the vector field f not in Hopf normal form). Then, it is trivial to verify (see the details in Appendix B.2) that close to the BH ($\alpha = 0$) the SH orbit cannot exist in the linearized system (3.7) (see Figure 4(left)), as the orbit starting at the tangency point $T^{(l)}$ comes back to $T^{(l)}$ itself (the linear system is a center). This also shows that the transition BF_2–BF_5 is generically not possible, as anticipated in section 2.1.

As for the GR bifurcation, the cycle exists for $\beta_2 > 0$ ($\beta_2 < 0$) (and is stable (unstable)) if the Hopf is super(sub)-critical (negative (positive) l_1^0 in (BH.5)) and is geometrically a circle of radius $\sqrt{-\beta_2/l_1^0} + O(\beta_2)$ (where $O(\beta_2)$-terms are smooth functions of β_1). Let $\sigma(\beta)$ be the distance of the equilibrium $y = 0$ from the discontinuity boundary, with positive (negative) values if $H(0, \alpha(\beta))$ is negative (positive), in order to make $\sigma(\beta)$ differentiable at $\beta = 0$. Thanks to (G.1), (G.3), and to our choice of β_1, we can write σ as

$$\sigma(\beta) = \sigma^0_{\beta_1}\beta_1 + O(\|\beta\|^2), \tag{3.21}$$

where $\sigma^0_{\beta_1}$ is computed in Appendix D and shown to be generically nonzero (see (D.5)).

The asymptotic of the GR bifurcation curve (GR_1 (GR_2) if $l_1^0 < 0$ ($l_1^0 > 0$) in (BH.5)) is obtained by equating the radius of the cycle with the distance σ and by eliminating nonleading terms, i.e.,

$$\sqrt{-\beta_2/l_1^0} \simeq \sigma^0_{\beta_1}\beta_1. \tag{3.22}$$

The GR curve hence emanates from $\beta = 0$ tangentially to the β_1-axis (the Hopf curve) with positive β_1 (the equilibrium $y = 0$ is admissible) and positive $-\beta_2/l_1^0$.

A quadratic asymptotic in the original α-parameter plane requires the expansion of the parameter change (3.3) and (3.20) up to second-order terms, and reads

$$\begin{aligned} 0 \simeq\ & \frac{\beta^0_{2\alpha_1}}{l_1^0}\alpha_1 + \frac{\beta^0_{2\alpha_2}}{l_1^0}\alpha_2 \\ & + \left((\sigma^0_{\beta_1}\beta^0_{1\alpha_1})^2 + \frac{\beta^0_{2\alpha_1^2}}{2l_1^0}\right)\alpha_1^2 + \left(2(\sigma^0_{\beta_1})^2\beta^0_{1\alpha_1}\beta^0_{1\alpha_2} + \frac{\beta^0_{2\alpha_1\alpha_2}}{l_1^0}\right)\alpha_1\alpha_2 + \left((\sigma^0_{\beta_1}\beta^0_{1\alpha_2})^2 + \frac{\beta^0_{2\alpha_2^2}}{2l_1^0}\right)\alpha_2^2, \end{aligned} \tag{3.23}$$

where $\beta^0_{1\alpha} = -\tau^0_{2\alpha}$ and $\beta^0_{2\alpha} = \mu^0_\alpha/\omega^0$ (see the second equation of (A.5) for an explicit expression for $\tau^0_{2\alpha}$).

In conclusion, we have proved the following result.

Theorem BH. *Suppose that for a planar Filippov system* (1.1) *the following assumptions hold at* $\alpha = 0$:

(BH.1) *the vector field* $f^{(1)}$ *has an equilibrium at* $x = 0$ *lying on* Σ *and having purely imaginary eigenvalues, i.e.,* $(f^{(1)})^0 = 0$, $H^0 = 0$, $\operatorname{Re}\lambda^0_{1,2} = \pm i\omega \neq 0$;

(G.2) *the vector field* $f^{(2)}$ *is transverse to* Σ *at* $x = 0$, *i.e.,* $H^0_x(f^{(2)})^0 \neq 0$;

(G.3) *the BE bifurcation is locally well defined, i.e.,* $H^0_\alpha \neq 0$;

(G.4) *the BE exhibits a generic scenario, i.e.,* $H^0_x((f^{(1)}_x)^0)^{-1}(f^{(2)})^0 \neq 0$;

(BH.5) *the Hopf bifurcation is locally well defined and generic, i.e.,* $\mu^0_\alpha \neq 0$ *and* $l^0_1 \neq 0$;

(BH.6) *the Hopf and BE bifurcation curves are transversal, i.e.,* $\langle (H^\perp_\alpha)^0, \mu^0_\alpha \rangle \neq 0$.

Then, by applying a smooth and invertible transformation of coordinate and parameters, $y = y(x, \alpha)$ *and* $\beta = \beta(\alpha)$, *and a time reparametrization, system* (1.1) *can be reduced to the canonical form*

$$\dot y = \begin{cases} \begin{bmatrix} \beta_2 & -1 \\ 1 & \beta_2 \end{bmatrix} y + l_1(\beta)\|y\|^2 y + O(\|y^4\|), & y_2 < \beta_1(1 + O(\|\beta\|)) + O(\|y^2\|), \\ v(\beta) + O(\|y\|), & y_2 > \beta_1(1 + O(\|\beta\|)) + O(\|y^2\|), \end{cases}$$

where, independently on O*-terms, locally to* $\beta = 0$, *the* β_2*-axis is the BE bifurcation, the positive* β_1*-semiaxis is the Hopf bifurcation, and a grazing bifurcation emanates from* $\beta = 0$ *tangentially to the Hopf with asymptotic* (3.22) ((3.23) *in the original parameters*). *No other bifurcation is rooted at* $\beta = 0$.

The bifurcation diagrams of the BH singularity locally to $\beta = 0$ are reported in Figure 6. Generically, there are four cases, depending on whether the Hopf bifurcation is super- or subcritical ($l^0_1 \lessgtr 0$ in (BH.5), left/right panels in the figure) and on the BE scenario, persistence or nonsmooth-fold (positive/negative sign in (G.4), top/bottom). For uniformity with the rest of the paper, the state portraits are presented with reference to the canonical form (3.1), where the vector field f is not in Hopf normal form.

4. Example: On-off harvesting control of a prey-predator ecosystem. We apply our results to the 2D ecological example studied in [20] (see also [11]). It describes a two-population community, a prey and a predator with densities x_1 and x_2, respectively, where the predator population is harvested only when abundant, i.e., when $x_2 > \alpha$, α being a prescribed threshold.

The system's equations are

$$\dot x_1 = x_1(1 - x_1) - \frac{a x_1}{b + x_1} x_2, \tag{4.1a}$$

$$\dot x_2 = \frac{a x_1}{b + x_1} x_2 - d x_2, \tag{4.1b}$$

in S_1, where $x_2 < \alpha$ (the prey grows logistically in the absence of predators; predation rate follows the Holling type-II functional response—the Rosenzweig–MacArthur model—see, e.g., [23]), while an extra mortality term $-Ex_2$ due to harvesting is added to (4.1b) in S_2.

The bifurcation analysis of model (4.1) performed in [20] was limited to codim 1 bifurcations, but revealed several codim 2 points as intersections or terminating points of codim 1 bifurcation curves. In particular, the HBF and BH singularities are both identifiable in the parameter plane (α, b) (see points B and A in Figure 29 in [20]; other parameter values: $a = 0.3556$, $d = 0.04444$, $E = 0.2067$). We now apply the results of sections 3.2 and 3.3 locally to the HBF and BH bifurcations, with parameters (α, b) playing the role of (α_1, α_2).

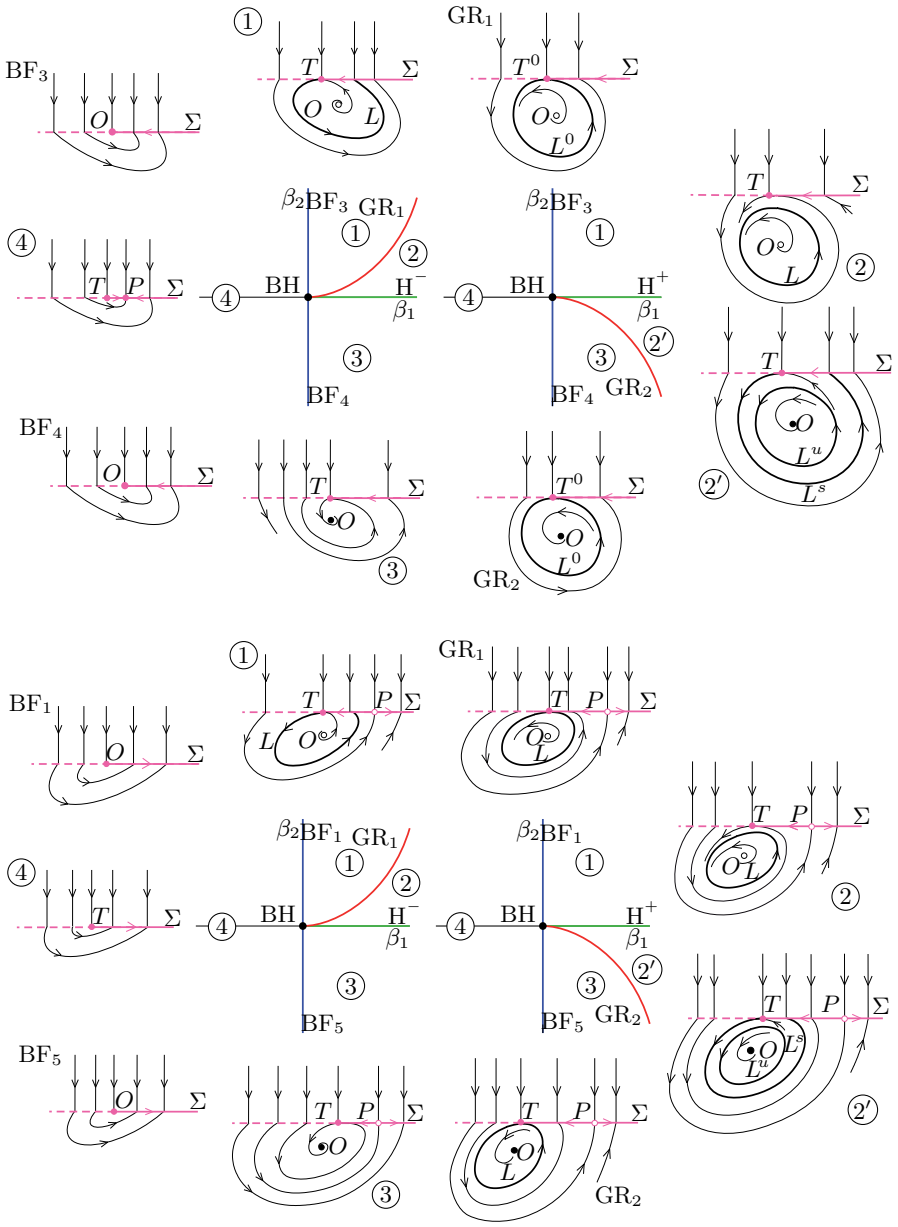

Figure 6. BH *universal local bifurcation diagrams (top (bottom): persistence (nonsmooth-fold) BE scenario; left (right): super(sub)-critical Hopf).*

Table 1 reports the parameter values (α^0, b^0) of the codim 2 point, the coordinates x^0 of the corresponding boundary equilibria, the values of the genericity conditions, and the bifurcation asymptotics; see the first two columns for the HBF and BH bifurcations found in [20]. Note that condition (G.4) is not satisfied, so that the BH case is degenerate. A change of BE scenario, from persistence to nonsmooth-fold (generalized BE; see [10]), occurs together with the BH; see (2.2). Although the asymptotic (3.23) remains valid, a fold bifurcation

Table 1

Numerical analysis of the HBF and BH bifurcations in model (4.1). The $*$-superscript refers to the modified model with parameter $p = 0.1$.

	HBF	BH	BH*
(α^0, b^0)	(0.9754, 0.3179)	(2.2225, 0.7780)	(2.2336, 0.7780)
x^0	(0.0454, 0.9753)	(0.1109, 2.2225)	(0.1110, 2.2225)
(G.1) / (BH.1)	$0, 0, (0.0369, 0.0369)$	$(0, 0, \pm 0.1859i)$	$(0, 0, \pm 0.1859i)$
(G.2)	-0.2016	-0.4594	-0.4595
(G.3)	$(-1, 2.9219)$	$(-1, 2.5)$	$(-1, 2.5143)$
(G.4) / (HBF.4)	-0.4013	0	-0.0591
(HBF.5) / (BH.5)	-0.1430	$((0, -0.0802), -0.1633)$	$((0, -0.0802), -0.1633)$
(HBF.6) / (BH.6)	(0, 21.8495)	-0.0802	-0.0802
SH and GR asymptotics			
SH:	$\alpha_1 - 3.8590\,\alpha_2 \simeq 0$		
GR:	$1.2507\,\alpha_2 + \alpha_1^2 - 5\,\alpha_1\alpha_2 + 13.7982\,\alpha_2^2 \simeq 0$		
GR*:	$1.2514\,\alpha_2 + \alpha_1^2 - 5.0286\,\alpha_1\alpha_2 + 13.8741\,\alpha_2^2 \simeq 0$		

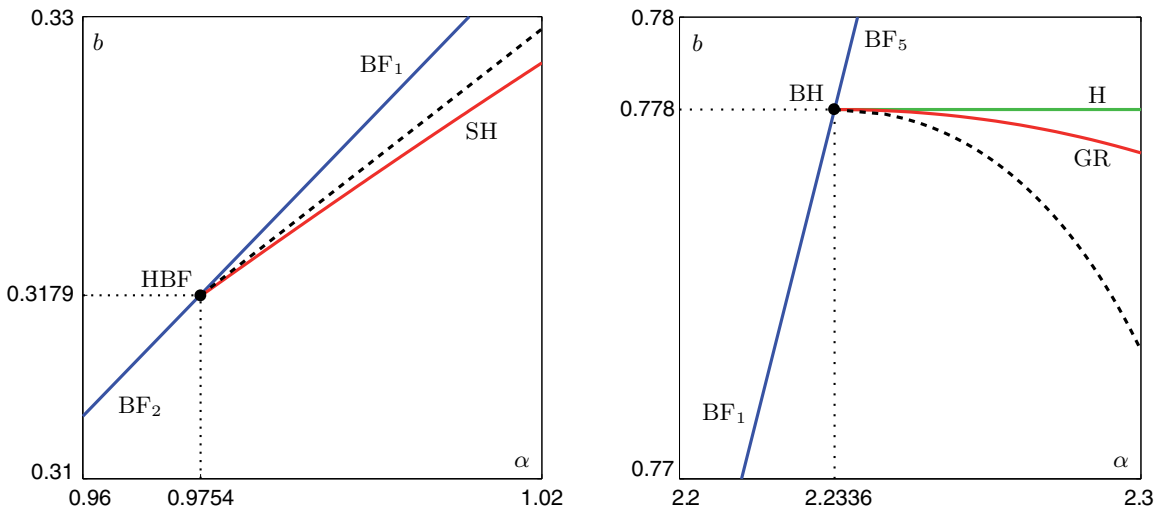

Figure 7. *Local bifurcation diagrams. Left:* HBF *bifurcation in the original model (4.1); right:* BH *bifurcation in the modified model (parameter $p = 0.1$). Black dashed curves:* SH *(left) and* GR *(right) asymptotics; see (3.18) and (3.23), respectively.*

between pseudoequilibria also emanates from the BH point tangentially to the BF curve (see curve PSN emanating from point A in Figure 29 in [20]), as indeed expected at a generalized BE [10].

In order to have a generic BH bifurcation, we have tilted the discontinuity boundary by considering system (4.1) when $x_2 < \alpha - p x_1$, $p = 0.1$ being a new parameter. This corresponds to a harvesting threshold that decreases with the prey abundance (up to zero, and remains zero for prey abundances higher than α/p). The last column in Table 1 reports the results of the generic BH bifurcation, and Figure 7 shows the two local bifurcation diagrams corresponding to the HBF case in the original model (left) and to the generic BH case (right). The asymptotics (3.18) and (3.23) are also reported (black dashed curves).

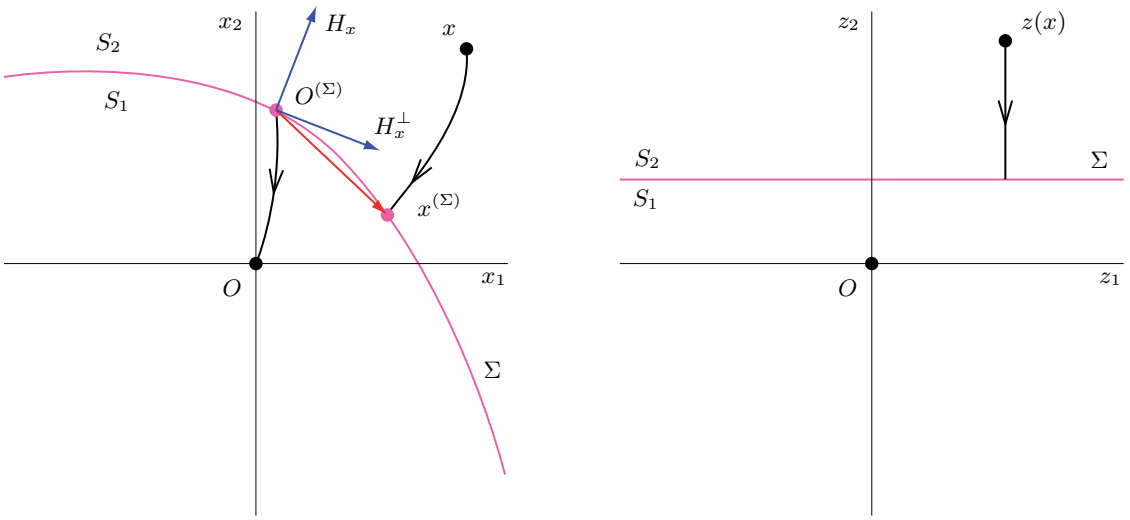

Figure 8. *The change of variables $z = z(x, \alpha)$.*

All the results in Table 1 have been computed with the two *Mathematica* scripts accompanying the paper (see 81254_01.zip [local/web 30.1KB]). By simply changing the system's definition and the values of the boundary equilibrium and of the parameters, the scripts can be reused on other systems. The bifurcation curves in Figure 7 have been computed with the package *SlideCont* [12].

Appendix A. The transformation $z = z(x, \alpha)$ reducing (1.1) to (3.1).

A.1. The transformation. Consider system (1.1) for (x, α) close to a BE bifurcation of the vector field $f^{(1)}$ at $(x, \alpha) = (0, 0)$, and assume (G.1), (G.2), and the parameter-dependent translation ensuring (2.1).

Let $x(t) = \Phi^{(2)}(x(0), t, \alpha)$ be the flow generated by the vector field $f^{(2)}$. Under (G.2), locally to $(x, \alpha) = (0, 0)$, the time $\tau_2(x, \alpha)$ needed by $\Phi^{(2)}$ to go from x to the discontinuity boundary Σ is implicitly defined by

$$H(\Phi^{(2)}(x, \tau_2(x, \alpha), \alpha), \alpha) = 0. \tag{A.1}$$

Note that $\tau_2(x, \alpha) = 0$ when x is on Σ and that, when sliding is stable (i.e., $H_x^0(f^{(2)})^0 < 0$ in (G.2)), $\tau_2(x, \alpha)$ is positive (negative) when $x \in S_2$ (S_1).

Let

$$x^{(\Sigma)}(x, \alpha) = \Phi^{(2)}(x, \tau_2(x, \alpha), \alpha) \quad \text{and} \quad O^{(\Sigma)}(\alpha) = \Phi^{(2)}(0, \tau_2(0, \alpha), \alpha),$$

and introduce the new variables z_1 and z_2 as follows (see Figure 8):

$$z_1 = z_1(x, \alpha) := \langle H_x^\perp(O^{(\Sigma)}(\alpha), \alpha),\ x^{(\Sigma)}(x, \alpha) - O^{(\Sigma)}(\alpha)\rangle, \tag{A.2a}$$

$$z_2 = z_2(x, \alpha) := \tau_2(x, \alpha) - \tau_2(0, \alpha). \tag{A.2b}$$

The variable change (A.2) maps $x = 0$ into $z = 0$ for any small $\|\alpha\|$ and is invertible close to $(x, \alpha) = (0, 0)$. In fact, z_1 is a local coordinate on Σ, with origin at $O^{(\Sigma)}$ and positive direction

along $H_x^\perp$, so that locally to $(z_1,\alpha)=(0,0)$ the vector $x^{(\Sigma)}(x,\alpha)-O^{(\Sigma)}(\alpha)$ (red in the figure) is a smooth function of z_1 and α, say $\chi(z_1,\alpha)$, and we can write

$$z^{-1}(z,\alpha)=x(z,\alpha)=\Phi^{(2)}(O^{(\Sigma)}(\alpha)+\chi(z_1,\alpha),-(z_2+\tau_2(0,\alpha)),\alpha).$$

Note that if also

$$z_0=\langle H_x(O^{(\Sigma)}(\alpha),\alpha),x^{(\Sigma)}(x,\alpha)-O^{(\Sigma)}(\alpha)\rangle$$

is stored together with z_1 and z_2, then the function χ can be computed as

$$\chi(z_1,\alpha)=\begin{bmatrix} H_x(O^{(\Sigma)}(\alpha),\alpha)\\ H_x^\perp(O^{(\Sigma)}(\alpha),\alpha)\end{bmatrix}^{-1}\begin{bmatrix} z_0\\ z_1\end{bmatrix}.$$

When x is on Σ, the equation of the discontinuity boundary in the new variables is simply $z_2=-\tau_2(0,\alpha)$ (i.e., the boundary is flat and horizontal, while z is above (below) the boundary when $x\in S_2$ (S_1)).

When $x\in S_2$, all points of the $f^{(2)}$-orbit starting at x reach the same point on Σ and therefore give the same value for z_1; i.e., the new vector field in S_2 is vertical. Moreover, it obviously results in

$$\dot z_2=\tau_{2x}(x,\alpha)\,f^{(2)}(x,\alpha)=-1, \tag{A.3}$$

since the time to reach Σ along the $f^{(2)}$-orbit (i.e., $z_2+\tau_2(0,\alpha)$; see (A.2b)) reduces by one unit in a unit of time. In formulas, by differentiating (A.1) w.r.t. x, we get

$$\tau_{2x}(x,\alpha)=-\frac{H_x(x^{(\Sigma)}(x,\alpha),\alpha)\Phi_x^{(2)}(x,\tau_2(x,\alpha),\alpha)}{H_x(x^{(\Sigma)}(x,\alpha),\alpha)f^{(2)}(x^{(\Sigma)}(x,\alpha),\alpha)},$$

where the product $\Phi_x^{(2)}(x,\tau_2(x,\alpha),\alpha)\,f^{(2)}(x,\alpha)$ in (A.3) is nothing but $f^{(2)}(x^{(\Sigma)}(x,\alpha),\alpha)$ (the first-order perturbation of the orbit's terminal point $x^{(\Sigma)}(x,\alpha)$ induced by perturbing the initial state x by $f^{(2)}(x,\alpha)$). In conclusion, we have $\dot z=[0,\,-1]^\top$ for $z\in S_2$.

When $x\in S_1$,

$$\dot z=f(z,\alpha):=z_x(x(z,\alpha),\alpha)f^{(1)}(x(z,\alpha),\alpha), \tag{A.4}$$

which defines the function f introduced in system (3.1).

Note that a similar change of variables can be defined for n-dimensional Filippov systems, provided that $(z_1,\dots,z_{n-1})$ define coordinates on Σ locally to $O^{(\Sigma)}$ (e.g., the scalar products with a base on the linear manifold tangent to Σ at $O^{(\Sigma)}$).

A.2. Useful derivatives. We now compute a few derivatives that are needed throughout the paper. They are evaluated at $x=0$ on the BE bifurcation curve (i.e., when $H(0,\alpha)=0$) if the argument α is present, or at $(x,\alpha)=(0,0)$ when the 0-superscript is used.

We start with function τ_2. From (A.1) it easily follows that

$$\tau_{2x}(0,\alpha)=-\frac{H_x(0,\alpha)}{H_x(0,\alpha)f^{(2)}(0,\alpha)},\quad \tau_{2\alpha}(0,\alpha)=-\frac{H_\alpha(0,\alpha)}{H_x(0,\alpha)f^{(2)}(0,\alpha)}, \tag{A.5}$$

$$\tau^0_{2xx_{1,2}} = -\left(H^0_{xx_{1,2}}\left(I + (f^{(2)})^0\tau^0_{2x}\right)\right.$$
$$\left. + H^0_x\left((f^{(2)}_x)^0\tau^0_{2x_{1,2}} + (f^{(2)}_{x_{1,2}})^0\tau^0_{2x} + (f^{(2)}_x)^0(f^{(2)})^0\tau^0_{2x}\tau^0_{2x_{1,2}}\right)\right) \Big/ \left(H^0_x(f^{(2)})^0\right), \tag{A.6}$$

and

$$\tau^0_{2x\alpha_{1,2}} = -\frac{H^0_{x\alpha_{1,2}}}{H^0_x(f^{(2)})^0} + \frac{H^0_x}{(H^0_x(f^{(2)})^0)^2}\left(H^0_{x\alpha_{1,2}}(f^{(2)})^0 + H^0_x(f^{(2)}_{\alpha_{1,2}})^0\right), \tag{A.7}$$

where H_x and τ_{2x} are (as usual) treated as row vectors and the denominators are nonzero for small $\|\alpha\|$ thanks to (G.2).

As for the change of variables $z = z(x,\alpha)$, from (A.2) we have

$$z_x(0,\alpha) = \begin{bmatrix} H^\perp_x(0,\alpha)\left(I + f^{(2)}(0,\alpha)\tau_{2x}(0,\alpha)\right) \\ \tau_{2x}(0,\alpha) \end{bmatrix}, \tag{A.8}$$

(A.9)
$$z^0_{xx_{1,2}} = \begin{bmatrix} 2(H^\perp_x)^0_{x_{1,2}}\left(I + (f^{(2)})^0\tau^0_{2x}\right) \\ \quad + (H^\perp_x)^0\left((f^{(2)}_x)^0\tau^0_{2x_{1,2}} + (f^{(2)}_{x_{1,2}})^0\tau^0_{2x} + (f^{(2)}_x)^0(f^{(2)})^0\tau^0_{2x}\tau^0_{2x_{1,2}} + (f^{(2)})^0\tau^0_{2xx_{1,2}}\right) \\ \tau^0_{2xx_{1,2}} \end{bmatrix},$$

$$z^0_{x\alpha_{1,2}} = \begin{bmatrix} (H^\perp_x)^0_{\alpha_{1,2}}\left(I + (f^{(2)})^0\tau^0_{2x}\right) + (H^\perp_x)^0\left((f^{(2)}_{\alpha_{1,2}})^0\tau^0_{2x} + (f^{(2)})^0\tau^0_{2x}\right) \\ \tau^0_{2x\alpha_{1,2}} \end{bmatrix}, \tag{A.10}$$

while by differentiating the identity $z(x(z,\alpha),\alpha) = z$, we get

$$x_z(0,\alpha) = z_x(0,\alpha)^{-1},\ \ x^0_{z\alpha_{1,2}} = -(z^0_x)^{-1}z^0_{x\alpha_{1,2}}(z^0_x)^{-1},\ \ x^0_{zz_{1,2}} = -(z^0_x)^{-1}z^0_{xx}\left(z^0_{x_{1,2}}, z^0_x\right), \tag{A.11}$$

where the bilinear operator z_{xx} can easily be obtained from (A.9).

Finally, the Jacobian of f at $z = 0$ introduced in (3.2) is given by

$$f_z(0,\alpha) = J(\alpha) = z_x(0,\alpha)f^{(1)}_x(0,\alpha)(z_x(0,\alpha))^{-1}, \text{ with } J^0 = z^0_x(f^{(1)}_x)^0x^0_z, \tag{A.12}$$

while the second derivatives are

$$f^0_{zz_{1,2}} = z^0_{xx}\left(x^0_z, (f^{(1)}_x)^0x^0_{z_{1,2}}\right) + z^0_{xx}\left(x^0_{z_{1,2}}, (f^{(1)}_x)^0x^0_z\right) + z^0_x(f^{(1)}_{xx})^0\left(x^0_{z_{1,2}}, x^0_z\right) + z^0_x(f^{(1)}_x)^0x^0_{zz_{1,2}} \tag{A.13}$$

and

$$f^0_{z\alpha_{1,2}} = J^0_{\alpha_{1,2}} = z^0_{x\alpha_{1,2}}(f^{(1)}_x)^0x^0_z + z^0_x(f^{(1)}_{x\alpha_{1,2}})^0x^0_z + z^0_x(f^{(1)}_x)^0x^0_{z\alpha_{1,2}}, \tag{A.14}$$

where (A.11) must be taken into account.

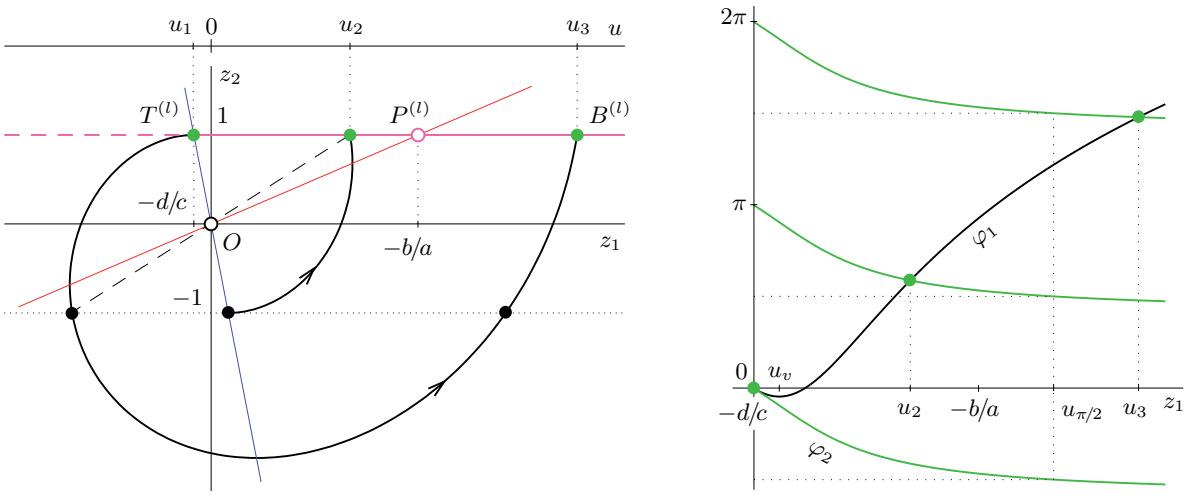

Figure 9. *Construction of function* $\psi(z_1, \alpha)$ *in* (3.10).

Appendix B. Derivation of the function ψ in (3.10).

B.1. The case $a + d \neq 0$. Consider the linear system (3.7), and replace z_1 with the new variable u measuring the slope of vector z w.r.t. axis z_2, i.e., $z_1 = u\, z_2$; see the left panel in Figure 9 (this trick is taken from [14, p. 246]). Then, we have

$$\frac{\dot z_1}{\dot z_2} = \frac{au + b}{cu + d} = \dot u \frac{z_2}{\dot z_2} + u, \tag{B.1}$$

which is solvable in the variables (u, z_2) by separation and yields

$$-\frac{1}{2}\log|-cu^2 + (a-d)u + b| + \frac{a+d}{2\omega}\left(\arctan\left(\frac{-2cu + a - d}{2\omega}\right) + k\pi\right) = \log|z_2| + C, \tag{B.2}$$

where $\omega = \sqrt{-\Delta}/2$ ($\Delta = (a-d)^2 + 4\,b\,c$ is defined in (3.4)), $k = 0, \pm 1, \pm 2, \ldots$ identifies smooth pieces of the solution with $u \to \pm\infty$ corresponding to $z_1 \to u\,\mathrm{sign}\, z_2$, and C is an arbitrarily constant. In order to consider all pieces as a whole, we apply (after some algebra) the tan function on both sides of (B.2) and get

$$\tan\left(\frac{\omega}{a+d}\log\left(z_2^2|-cu^2 + (a-d)u + b|C'\right)\right) = \frac{-2cu + a - d}{2\omega}, \tag{B.3}$$

where C' is a different constant, set by the initial condition

$$z_1(0) = u(0) = -d/c, \quad z_2(0) = 1, \tag{B.4}$$

i.e.,

$$\tan\left(\frac{\omega}{a+d}\log\left(\left|-\frac{ad}{c} + b\right| C'\right)\right) = \frac{a+d}{2\omega}. \tag{B.5}$$

In order to eliminate C', let us write (B.3) as

$$\tan\left(\frac{\omega}{a+d}\log\left(\left|-\frac{ad}{c}+b\right|C'\right)+\frac{\omega}{a+d}\log\left(z_2^2\frac{-cu^2+(a-d)u+b}{-ad/c+b}\right)\right)=\frac{-2cu+a-d}{2\omega},$$

where the absolute value in the second log has been removed because, under (HBF.5) and (3.5), the argument is a positive upward parabola in u: the numerator is a downward parabola with vertex at

$$u=u_v:=(a-d)/2c,\quad \text{with}\quad u_v-(-d/c)=(a+d)/(2c)>0, \tag{B.6}$$

and negative maximum $(a-d)^2/4c+b$, and the denominator is constant and negative; see (3.6). Now, exploiting (B.5) and that $\tan(\theta_1+\theta_2)=(\tan\theta_1+\tan\theta_2)/(1-\tan\theta_1\tan\theta_2)$, we get, after some algebra,

$$\tan\left(\frac{\omega}{a+d}\log\left(z_2^2\frac{-cu^2+(a-d)u+b}{-ad/c+b}\right)\right)=\frac{2\omega(cu+d)}{c(a+d)u+2bc-d(a-d)}. \tag{B.7}$$

We are interested in the solutions of (B.7) with $z_2=1$ (return to the discontinuity boundary), so we can set $z_1=u$, and we like to distinguish among different return points, so we go back to the arctan formulation and define

$$\begin{aligned}\psi_k(z_1,\alpha):=&\frac{\omega}{a+d}\log\left(\frac{-cz_1^2+(a-d)z_1+b}{-ad/c+b}\right)\\&-\arctan\left(c(a+d)z_1+2bc-d(a-d),2\omega(cz_1+d)\right)-k\pi,\end{aligned} \tag{B.8}$$

where the two-argument $\arctan(p_1,p_2)$ (often called atan2) gives here the angle of point (p_1,p_2) in $(-\pi,\pi]$, and the α-dependence is confined in a, b, c, d, and ω. Note that due to (HBF.5) and (3.5), the $p_{1,2}$-arguments in (B.8) are both linearly increasing with z_1, p_1 starting from a negative value $(-2\det J)$ at $z_1=-d/c$ and changing sign at

$$z_1=u_{\pi/2}:=(d(a-d)-2bc)/c(a+d),\quad \text{with}\quad u_{\pi/2}-u_v=-\Delta/(2c\,\mathrm{tr}J)>0, \tag{B.9}$$

while p_2 vanishes at $z_1=-d/c$. Hence, the two-argument arctan avoids the π-jump of the standard arctan at $z_1=u_{\pi/2}$, where $\arctan(0,p_2)$ with $p_2>0$ is continuous and gives $\pi/2$.

We now study the solutions $\tilde z_1$ such that $\psi_k(\tilde z_1,\alpha)=0$ for some k and show that $\tilde z_1=B_1^{(l)}(\alpha)$ (the z_1-value of the first return point $B^{(l)}(\alpha)$ to the boundary $z_2=1$ of the orbit of system (3.7) starting at (B.4); see Figure 9(left)) is the only solution for $k=1$ and $z_1\ge -d/c$. We therefore conclude that function ψ in (3.10) is defined by

$$\psi(z_1,\alpha):=\psi_1(z_1,\alpha),\quad z_1\ge -d/c. \tag{B.10}$$

The following is a sketch of the proof. We study the graphs of

$$\varphi_1(z_1,\alpha):=\frac{\omega}{a+d}\log\left(\frac{-cz_1^2+(a-d)z_1+b}{-ad/c+b}\right)$$

and

$$\varphi_2(z_1,\alpha):=\arctan\left(c(a+d)z_1+2bc-d(a-d),2\omega(cz_1+d)\right)-\pi,$$

where

$$\psi_k(z_1,\alpha)=\varphi_1(z_1,\alpha)-(\varphi_2(z_1,\alpha)+(k+1)\pi).$$

1. Due to the z_2^2-term in (B.3), values $\tilde{z}_1$ corresponding to points $(\tilde{z}_1, -1)$ of the orbit of system (3.7) starting at (B.4) are also solutions, as well as $\tilde{z}_1$ corresponding to points $(\tilde{z}_1, \pm 1)$ of the orbit starting at $z_1(0) = d/c$, $z_2(0) = -1$ (see the green and black dots in Figure 9(left)). However, each solution corresponding to a point with $z_2 = -1$ matches a solution (of the other orbit) where $z_2 = 1$ (see the dashed segment in the figure), so we can consider only solutions corresponding to points of both orbits with $z_2 = 1$ (green dots), where indeed we can substitute u with z_1.
2. From Figure 9(left), it is clear that $B_1^{(l)}(\alpha)$ corresponds to the third solution $\tilde{z}_1$ encountered by considering any k and increasing z_1 starting from $z_1 = -d/c$.
3. $\varphi_1(-d/c, \alpha) = \varphi_2(-d/c, \alpha) = 0$, so that $\tilde{z}_1 = -d/c$ is a solution for $k = -1$.
4. $\varphi_{1z_1}(z_1, \alpha) = \frac{\omega}{a+d} \frac{-2cz_1+a-d}{-cz_1^2+(a-d)z_1+b}$, $\varphi_{2z_1}(z_1, \alpha) = \frac{\omega}{-cz_1^2+(a-d)z_1+b}$, and also $\varphi_{1z_1}(-d/c, \alpha) = \varphi_{2z_1}(-d/c, \alpha) = -c\omega/\det J < 0$ (due to equations (HBF.5) and (3.5)). Moreover, $\varphi_{1z_1}(-d/c, \alpha)/\varphi_{2z_1}(-d/c, \alpha) = (-2cz_1 + a - d)/(a + d)$ linearly goes from 1 to 0 for z_1 from $= -d/c$ to u_v (see (B.6)). Thus, $\varphi_{1,2}$ both decrease for $z_1 \in [-d/c, u_v]$, but φ_1 stays above φ_2 (see Figure 9(right)), so there are no other solutions for $k = -1$ in $[-d/c, u_v]$.
5. For $z_1 > u_v$, φ_1 is increasing, while φ_2 continues to decrease and tends to $\arctan(c(a+d), 2\omega c) - \pi$ as $z_1 \to \infty$, so $\tilde{z}_1 = -d/c$ is the only solution for $k = -1$.
6. For $k \neq -1$, there are no solutions in $[-d/c, u_v]$. In fact, since $u_v < u_{\pi/2}$ (see (B.9)), we have $0 \geq \varphi_1 \geq \varphi_2 > -\pi/2$, i.e., $\varphi_1 \in (-\pi/2, 0]$, while $\varphi_2 + (k+1)\pi \in ((k+1)\pi - \pi/2, (k+1)\pi]$.
7. For $k < -1$, there is no solution for $z_1 > u_v$, as φ_1 stays above φ_2 (see Figure 9(right)).
8. For $k > -1$, there is a unique solution for $z_1 > u_v$, as $\varphi_1(u_v, \alpha) < \varphi_2(u_v, \alpha) + (k+1)\pi$, φ_1 is increasing, and φ_2 is decreasing (see Figure 9(right)), so that (B.10) follows from point 2 above.

Finally, note that the test function (3.11) holds true also in the case of clockwise rotations ($b^0 > 0$ and $c^0 < 0$). Although a few details do change in the derivation (i.e., $u < -d/c$ is the interval of interest, $\psi(z_1, \alpha)$ is positive (negative) for z_1 smaller (larger) than $B_1^{(l)}$, and BF_1 (BF_2) is the case in which $B_1^{(l)}$ is greater (less) than $-b/a$), the final result does not depend on b and c independently, but only on their product.

B.2. The case $a + d = 0$. At a Hopf bifurcation, the solution (B.7) of (B.1) degenerates into

$$\log\left(z_2^2 \frac{-cu^2 + (a-d)u + b}{-ad/c + b}\right) = 0. \tag{B.11}$$

Setting $z_2 = 1$ (return to the discontinuity boundary from initial condition (B.4)), there is a unique solution at $u = -d/c$. (As discussed in section B.1, the log-argument is a positive upward parabola that, in the case $a + d = 0$, has the vertex at $u = u_v := -d/c$ (see (B.6)) and minimum value equal to 1.) Indeed, the linear system (3.7) is a center, and the elliptical orbit through (B.4) grazes the boundary $z_2 = 1$ exactly at (B.4). Thus, we simply have $\psi(z_1, \alpha) = z_1 + d(\alpha)/c(\alpha)$, i.e., $B^{(l)}(\alpha) = -d(\alpha)/c(\alpha)$.

Appendix C. Computation of s_{10}, s_{20}, and s_{11} in (3.16).

C.1. Computation of s_{10}.

From definition (3.15) it follows that

$$s_{\beta_1} = f_{1z}(\Phi_z T_{\beta_1} + \Phi_t \tau_{\beta_1} + \Phi_\alpha \alpha_{\beta_1}) + f_{1\alpha}\alpha_{\beta_1}, \tag{C.1}$$

where arguments are omitted for simplicity.

In order to evaluate (C.1) at $\beta = 0$, note that

$$\Phi^0_z = \exp(J^0\tau^0), \quad \Phi^0_t = f^0 = 0, \quad \Phi^0_\alpha = 0, \quad f^0_{1\alpha} = 0 \tag{C.2}$$

(due to (2.1)), that at the HBF bifurcation

$$\exp(J^0\tau^0)\begin{bmatrix} -d^0/c^0 \\ 1 \end{bmatrix} = \begin{bmatrix} -b^0/a^0 \\ 1 \end{bmatrix}$$

(the orbit of the linear system (3.7) starting at $T^{(l)}$ goes back in time τ^0 to the boundary Σ at $P^{(l)}$; see (3.8), (3.9), (3.14), and Figure 4(left)), and that from the definition

$$T(\beta) := [T_1(\beta),\, \beta_1]^\top, \quad f_2(T(\beta), \alpha(\beta)) = 0, \tag{C.3}$$

it follows that

$$T^0_{\beta_1} = [-d^0/c^0,\, 1]^\top \tag{C.4}$$

(here we use the 0-superscript also for evaluation at $(z, t, \beta) = (0, \tau^0, 0)$).

Then, from (C.1) we find

$$s_{10} = s^0_{\beta_1} = [a^0,\, b^0][-b^0/a^0,\, 1]^\top = 0.$$

C.2. Computation of s_{20}.

Taking the derivative of (C.1) w.r.t. β_1, evaluating at $\beta = 0$, and taking into account (C.2)–(C.4) and

$$\Phi^0_{zt} = J^0 \exp(J^0\tau^0), \quad \Phi^0_{tt} = \Phi^0_{t\alpha} = \Phi^0_{\alpha^2} = 0, \quad f^0_{1\alpha^2} = 0, \tag{C.5}$$

we get

$$\begin{aligned} s_{20} = s^0_{\beta_1^2} = {} & f^0_{1zz}\left(\begin{bmatrix} -b^0/a^0 \\ 1 \end{bmatrix}, \begin{bmatrix} -b^0/a^0 \\ 1 \end{bmatrix}\right) + 2[a^0_\alpha \alpha^0_{\beta_1},\, b^0_\alpha \alpha^0_{\beta_1}]\begin{bmatrix} -b^0/a^0 \\ 1 \end{bmatrix} + [a^0,\, b^0] \\ & \times \left(\Phi^0_{zz}\left(\begin{bmatrix} -d^0/c^0 \\ 1 \end{bmatrix}, \begin{bmatrix} -d^0/c^0 \\ 1 \end{bmatrix}\right) + 2J^0\begin{bmatrix} -b^0/a^0 \\ 1 \end{bmatrix}\tau^0_{\beta_1} + 2\Phi^0_{z\alpha}\alpha^0_{\beta_1}\begin{bmatrix} -d^0/c^0 \\ 1 \end{bmatrix} + \exp(J^0\tau^0)\, T^0_{\beta_1^2}\right), \end{aligned} \tag{C.6}$$

where

$$\alpha^0_\beta = [\alpha^0_{\beta_1},\, \alpha^0_{\beta_2}] = (\beta^0_\alpha)^{-1} = \frac{1}{-\tau^0_{2\alpha_1}\varphi^0_{\alpha_2} + \tau^0_{2\alpha_2}\varphi^0_{\alpha_1}}\begin{bmatrix} \varphi^0_{\alpha_2} & \tau^0_{2\alpha_2} \\ -\varphi^0_{\alpha_1} & -\tau^0_{2\alpha_1} \end{bmatrix} \tag{C.7}$$

from (3.3),

$$\Phi^0_{zz}(\cdot,\cdot) = \int_0^{\tau^0} \exp(J^0(\tau^0 - t))\, f^0_{zz}\big(\exp(J^0 t)(\cdot), \exp(J^0 t)(\cdot)\big)\, \mathrm{d}t$$

(by Picard iterations; see, e.g., [19, sect. 9.5.1]), and

$$\Phi^0_{z\alpha_{1,2}} = \int_0^{\tau^0} \exp(J^0(\tau^0 - t))\, J^0_{\alpha_{1,2}} \exp(J^0 t)\, \mathrm{d}t$$

(see, e.g., [1, sect. 10.14]), while from (C.3) we get

$$T^0_{1\beta_1^2} = -\frac{1}{c^0} f^0_{2zz}\left(\begin{bmatrix} -d^0/c^0 \\ 1 \end{bmatrix}, \begin{bmatrix} -d^0/c^0 \\ 1 \end{bmatrix}\right) - 2\frac{c^0 d^0_\alpha - c^0_\alpha d^0}{(c^0)^2}\alpha^0_{\beta_1}, \quad T^0_{2\beta_1^2} = 0.$$

(Expressions for f_{zz}, $\tau^0_{2\alpha}$, and for the elements a^0_α, b^0_α, c^0_α, d^0_α of J^0_α can be found in Appendix A.2, while the α-derivatives of φ can be obtained from the derivatives of φ w.r.t. a–d and from a^0_α–d^0_α.)

As for $\tau^0_{\beta_1}$, we need to take the second β_1-derivative of the definition (3.13). In fact, evaluating the first derivative

$$(\Phi_z T_{\beta_1} + \Phi_t \tau_{\beta_1} + \Phi_\alpha \alpha_{\beta_1})_2 = 1 \tag{C.8}$$

at $\beta = 0$ simply gives $1 = 1$, while one further differentiation gives

$$\tau_{\beta_1} = \frac{1}{b^0 c^0/a^0 - d^0}\left(\Phi^0_{zz}\left(\begin{bmatrix} -d^0/c^0 \\ 1 \end{bmatrix}, \begin{bmatrix} -d^0/c^0 \\ 1 \end{bmatrix}\right) + 2\Phi^0_{z\alpha}\alpha^0_{\beta_1}\begin{bmatrix} -d^0/c^0 \\ 1 \end{bmatrix} + \exp(J^0\tau^0)\, T^0_{\beta_1^2}\right)_2.$$

What we still need to evaluate (C.6) is an explicit formula for τ^0. For this we need to consider the coordinates y of z in the real eigenbasis of J^0, i.e., $y = Q^0 z$ with $(Q^0)^{-1} = [\mathrm{Re}\, q^0, -\mathrm{Im}\, q^0]$, q^0 being a complex eigenvector of J^0 associated to eigenvalue $(a^0+d^0)/2+i\omega^0$, e.g., $q^0 = [(a^0 - d^0)/(2c^0), 1]^\top + i[\omega^0/c^0, 0]^\top$. In the new coordinates, the flow generated by the linear system (3.7) at $\alpha = 0$ rotates counterclockwise at constant angular velocity ω^0, so that, at the HBF bifurcation, τ^0 is the angle spanned by the starting and end points $Q^0(T^{(l)})^0$ and $Q^0(P^{(l)})^0$ (see (3.8) and (3.9)) divided by ω^0, i.e.,

$$\tau^0 := \frac{1}{\omega^0}\left(2\pi - \arccos\left(\frac{\langle Q^0(T^{(l)})^0, Q^0(P^{(l)})^0\rangle}{\sqrt{\langle Q^0(T^{(l)})^0, Q^0(T^{(l)})^0\rangle\langle Q^0(P^{(l)})^0, Q^0(P^{(l)})^0\rangle}}\right)\right). \tag{C.9}$$

C.3. Computation of s_{11}. Taking the derivative of (C.1) w.r.t. β_2, evaluating at $\beta = 0$, and taking into account (C.2)–(C.5) and that $T^0_{\beta_2} = 0$ (easy to check from (C.3)), we get

$$\begin{aligned} s_{11} = s^0_{\beta_1\beta_2} &= [a^0_\alpha \alpha^0_{\beta_2}, b^0_\alpha \alpha^0_{\beta_2}]\begin{bmatrix} -b^0/a^0 \\ 1 \end{bmatrix} \\ &\quad + [a^0, b^0]\left(J^0\begin{bmatrix} -b^0/a^0 \\ 1 \end{bmatrix}\tau^0_{\beta_2} + \Phi^0_{z\alpha}\alpha^0_{\beta_2}\begin{bmatrix} -d^0/c^0 \\ 1 \end{bmatrix} + \exp(J^0\tau^0)\, T^0_{\beta_1\beta_2}\right), \end{aligned} \tag{C.10}$$

where, from (C.3), we have

$$T^0_{1\beta_1\beta_2} = -\frac{c^0 d^0_\alpha - c^0_\alpha d^0}{(c^0)^2}\alpha^0_{\beta_2}, \quad T^0_{2\beta_1\beta_2} = 0,$$

and $\alpha^0_{\beta_2}$ is the first column in (C.7).

Instead of computing $\tau^0_{\beta_2}$ directly, taking the β_2-derivative of (C.8), we note that near $\beta = 0$ we can write

$$\exp(J(\alpha(\beta))\tau(\beta)) \begin{bmatrix} -d(\alpha(\beta))/c(\alpha(\beta)) \\ 1 \end{bmatrix} = \begin{bmatrix} B_1^{(l)}(\alpha(\beta)) + \beta_1\zeta_1(\beta) \\ 1 + \beta_1\zeta_2(\beta) \end{bmatrix} \tag{C.11}$$

for some smooth function $\zeta(\beta)$ accounting for the fact that, when $\beta_1 \neq 0$, τ is different from the time $\tau^{(l)}$ required by the linear system (3.7) to go from $T^{(l)}$ back to the boundary $z_2 = 1$ at $z_1 = B_1^{(l)}$. Then, by taking the derivative of (C.11) w.r.t. β_2 at $\beta = 0$, and recalling from Appendix B.1 that $\psi(B_1^{(l)}(\alpha), \alpha) = 0$, we obtain an explicit expression for the terms involving $\tau^0_{\beta_2}$ and $\Phi^0_{z\alpha}$ in (C.10), i.e.,

$$\begin{aligned} J^0 \begin{bmatrix} -b^0/a^0 \\ 1 \end{bmatrix} \tau^0_{\beta_2} + \Phi^0_{z\alpha}\alpha^0_{\beta_2} \begin{bmatrix} -d^0/c^0 \\ 1 \end{bmatrix} \\ = \exp(J^0\tau^0) \begin{bmatrix} (c^0 d^0_\alpha - c^0_\alpha d^0)\alpha^0_{\beta_2}/(c^0)^2 \\ 0 \end{bmatrix} + \begin{bmatrix} -\psi^0_\alpha \alpha^0_{\beta_2}/\psi^0_{z_1} \\ 0 \end{bmatrix} \end{aligned} \tag{C.12}$$

(expressions for $\psi^0_{z_1}$ and ψ^0_α can be obtained from Appendix B.1). Substituting (C.12) into (C.10), we finally get

$$s_{11} = [a^0_\alpha \alpha^0_{\beta_2},\, b^0_\alpha \alpha^0_{\beta_2}] \begin{bmatrix} -b^0/a^0 \\ 1 \end{bmatrix} + [a^0,\, b^0] \begin{bmatrix} -\psi^0_\alpha \alpha^0_{\beta_2}/\psi^0_{z_1} \\ 0 \end{bmatrix}. \tag{C.13}$$

Expression (C.13) links s_{11} to our test function φ (defined in (3.10) and derived in Appendix B.1). Straightforward algebra indeed yields

$$s_{11} = -\frac{a^0}{\psi^0_{z_1}} \varphi^0_\alpha \alpha^0_{\beta_2},$$

which shows how genericity conditions (HBF.4) (i.e., $a^0 > 0$) and (HBF.6) imply $s_{11} \neq 0$. ($\psi^0_{z_1} \neq 0$ follows from the smoothness of φ.)

Appendix D. Computation of $\sigma^0_{\beta_1}$ in (3.21). Here we follow the approach introduced in [8] to study the grazing of an invariant curve close to a Border–Neimark–Sacker bifurcation in discrete time.

Introduce the complex variable $w = y_1 + iy_2$ used in [19, sect. 3.5] to describe the Hopf normal form, and write the inverse change of variables as $x = x(w, \bar{w}, \alpha)$ (the overbar stands for complex conjugation). From the normal form reduction, it follows that

$$x^0_w = q^0, \quad x^0_{\bar{w}} = \bar{q}^0, \tag{D.1}$$

where q^0 is the complex eigenvector of $(f_x^{(1)})^0$ associated with eigenvalue $+i\omega^0$, while (2.1) implies

$$x^0_\alpha = 0. \tag{D.2}$$

Then, due to (G.2) we have

$$H_y^0 = H_x^0 x_y^0 = 2H_x^0 \left[\operatorname{Re} q^0,\ -\operatorname{Im} q^0\right] \neq 0, \tag{D.3}$$

and we can define the angle of vector H_y^0 as

$$\theta_0 := \arctan(H_{y_1}^0, H_{y_2}^0) \tag{D.4}$$

(using the two-argument arctan in $(-\pi, \pi]$).

For θ in a neighborhood of θ_0, introduce axis r with origin at $y = 0$ and direction θ, so that positive (negative) values of r measure distances from $y = 0$ along the direction θ ($\theta + \pi$). Coordinates (r, θ) are like polar coordinates but allow differentiation w.r.t. r at $r = 0$. Locally to $(r, \theta) = (0, \theta_0)$ and $\beta = 0$, we can therefore express the discontinuity boundary Σ as

$$\Sigma := \{(r, \theta) : H(x(r\exp(i\theta), r\exp(-i\theta), \alpha(\beta)), \alpha(\beta)) = 0\},$$

where

$$\frac{d}{dr} H(x(r\exp(i\theta_0), r\exp(-i\theta_0), 0), 0)\Big|_{r=0} = 2H_x^0 \operatorname{Re}(q^0 \exp(i\theta_0)) = H_y^0 \begin{bmatrix} \cos(\theta_0) \\ \sin(\theta_0) \end{bmatrix} \neq 0$$

(see (D.3) and recall that H_y^0 is proportional to $[\cos(\theta_0), \sin(\theta_0)]^\top$ by definition of (D.4)), so that, by the implicit function theorem, we can represent Σ explicitly as $r = \delta(\theta, \beta)$, $\delta(\theta, 0) = 0$, for some smooth function δ defined for θ in an open neighborhood (θ', θ'') of θ_0.

Now, define $\theta_m(\beta) := \arg\min_{\theta \in (\theta', \theta'')} \{|\delta(\theta, \beta)|\}$ for $\beta \neq 0$, and note that $\lim_{\beta \to 0} \theta_m(\beta) = \theta_0$, so we can set $\theta_m^0 = \theta_0$. Then, the distance σ of the equilibrium $y = 0$ from Σ is given by

$$\sigma(\beta) := \delta(\theta_m(\beta), \beta),$$

with

$$\sigma_{\beta_1}^0 = \delta_{\beta_1}(\theta_0, 0) \tag{D.5a}$$

in (3.21) (recall that $\delta(\theta, 0) = 0$ for all $\theta \in (\theta', \theta'')$, so $\delta_\theta(\theta_0, 0) = 0$).

In order to compute $\delta_{\beta_1}(\theta_0, 0)$, consider the identity

$$H(x(\delta(\theta_0, \beta)\exp(i\theta_0), \delta(\theta_0, \beta)\exp(-i\theta_0), \alpha(\beta)), \alpha(\beta)) = 0,$$

and take the derivative w.r.t. β_1 at $\beta = 0$. We thus obtain

$$\delta_{\beta_1}(\theta_0, 0) = -\frac{H_x^0 (f^{(2)})^0}{H_x^0 \left[\operatorname{Re} q^0,\ -\operatorname{Im} q^0\right] \left[\begin{smallmatrix} \cos(\theta_0) \\ \sin(\theta_0) \end{smallmatrix}\right]}, \tag{D.5b}$$

where (D.1), (D.2),

$$\alpha_\beta^0 = (\beta_\alpha^0)^{-1} = \frac{\omega^0}{-\tau_{2\alpha_1}^0 \mu_{\alpha_2}^0 + \tau_{2\alpha_2}^0 \mu_{\alpha_1}^0} \begin{bmatrix} \mu_{\alpha_2}^0/\omega^0 & \tau_{2\alpha_2}^0 \\ -\mu_{\alpha_1}^0/\omega^0 & -\tau_{2\alpha_1}^0 \end{bmatrix}$$

from (3.20), and the second equation of (A.5) have been taken into account. Thanks to (G.2) and to the definitions in (D.3) and (D.4), we therefore have $\sigma_{\beta_1}^0 \neq 0$.

Acknowledgment. The authors would like to thank an anonymous reviewer for his useful and precise comments.

REFERENCES

[1] R. Bellman, *Introduction to Matrix Analysis*, 2nd ed., Classics in Appl. Math. 19, SIAM, Philadelphia, PA, 1997.

[2] M. di Bernardo, C. J. Budd, A. R. Champneys, and P. Kowalczyk, *Piecewise-Smooth Dynamical Systems: Theory and Applications*, Springer-Verlag, Berlin, 2008.

[3] M. di Bernardo, M. I. Feigin, S. J. Hogan, and M. E. Homer, *Local analysis of C-bifurcations in n-dimensional piecewise smooth dynamical systems*, Chaos Soliton. Fract., 10 (1999), pp. 1881–1908.

[4] M. di Bernardo, A. Nordmark, and G. Olivar, *Discontinuity-induced bifurcations of equilibria in piecewise-smooth and impacting dynamical systems*, Phys. D, 237 (2008), pp. 119–136.

[5] M. di Bernardo, D. J. Pagano, and E. Ponce, *Nonhyperbolic boundary equilibrium bifurcations in planar Filippov systems: A case study approach*, Internat. J. Bifur. Chaos Appl. Sci. Engrg., 18 (2008), pp. 1377–1392.

[6] M. di Bernardo, C. J. Budd, A. R. Champneys, P. Kowalczyk, A. B. Nordmark, G. Olivar Tost, and P. T. Piiroinen, *Bifurcations in nonsmooth dynamical systems*, SIAM Rev., 50 (2008), pp. 629–701.

[7] A. Colombo, P. Lamiani, L. Benadero, and M. di Bernardo, *Two-parameter bifurcation analysis of the buck converter*, SIAM J. Appl. Dyn. Syst., 8 (2009), pp. 1507–1522.

[8] A. Colombo and F. Dercole, *Discontinuity induced bifurcations of nonhyperbolic cycles in nonsmooth systems*, SIAM J. Appl. Dyn. Syst., 9 (2010), pp. 62–83.

[9] H. Dankowicz and X. Zhao, *Local analysis of co-dimension-one and co-dimension-two grazing bifurcations in impact microactuators*, Phys. D, 202 (2005), pp. 238–257.

[10] F. Della Rossa and F. Dercole, *Generalized boundary equilibria in n-dimensional Filippov systems: The transition between persistence and nonsmooth-fold scenarios*, Phys. D, to appear.

[11] F. Dercole, A. Gragnani, Yu. A. Kuznetsov, and S. Rinaldi, *Numerical sliding bifurcation analysis: An application to a relay control system*, IEEE Trans. Circuits-I, 50 (2003), pp. 1058–1063.

[12] F. Dercole and Yu. A. Kuznetsov, *SlideCont: An Auto97 driver for bifurcation analysis of Filippov systems*, ACM Trans. Math. Software, 31 (2005), pp. 95–119.

[13] A. F. Filippov, *Differential equations with discontinuous right-hand side*, in Amer. Math. Soc. Transl. Ser. 2, American Mathematical Society, Providence, RI, 1964, pp. 199–231.

[14] A. F. Filippov, *Differential Equations with Discontinuous Righthand Sides*, Kluwer Academic Publishers, Dordrecht, The Netherlands, 1988.

[15] M. Guardia, T. M. Seara, and M. A. Teixeira, *Generic bifurcations of low codimension of planar Filippov systems*, J. Differential Equations, 250 (2011), pp. 1967–2023.

[16] P. Kowalczyk and M. di Bernardo, *Two-parameter degenerate sliding bifurcations in Filippov systems*, Phys. D, 204 (2005), pp. 204–229.

[17] P. Kowalczyk, M. di Bernardo, A. R. Champneys, S. J. Hogan, M. Homer, P. T. Piiroinen, Yu. A. Kuznetsov, and A. Nordmark, *Two-parameter discontinuity-induced bifurcations of limit cycles: Classification and open problems*, Internat. J. Bifur. Chaos Appl. Sci. Engrg., 16 (2006), pp. 601–629.

[18] P. Kowalczyk and P. T. Piiroinen, *Two-parameter sliding bifurcations of periodic solutions in a dry-friction oscillator*, Phys. D, 237 (2008), pp. 1053–1073.

[19] Yu. A. Kuznetsov, *Elements of Applied Bifurcation Theory*, 3rd ed., Springer-Verlag, Berlin, 2004.

[20] Yu. A. Kuznetsov, S. Rinaldi, and A. Gragnani, *One-parameter bifurcations in planar Filippov systems*, Internat. J. Bifur. Chaos Appl. Sci. Engrg., 13 (2003), pp. 2157–2188.

[21] J. F. Mason and P. T. Piiroinen, *The effect of codimension-two bifurcations on the global dynamics of a gear model*, SIAM J. Appl. Dyn. Syst., 8 (2009), pp. 1694–1711.

[22] A. B. Nordmark and P. Kowalczyk, *A codimension-two scenario of sliding solutions in grazing-sliding bifurcations*, Nonlinearity, 19 (2006), pp. 1–26.

[23] H. R. Thieme, *Mathematics in Population Biology*, Princeton University Press, Princeton, NJ, 2003.